Archives of Computational Methods in Engineering
https://doi.org/10.1007/s11831-025-10331-7

RESEARCH

Exploration of Different Soliton Solutions for the Stochastic Davey–Stewartson Model Under the Influence of Noise

Fatma Nur Kaya Sağlam[1] · Bahadır Kopçasız[2] · Karim K. Ahmed[3]

Received: 8 June 2025 / Revised: 23 July 2025 / Accepted: 12 August 2025

Abstract

In this paper, we research the stochastic Davey–Stewartson (SDS) mathematical model, which is crucial in modeling a broad variety of physical processes such as surface and internal wave propagation in hydrodynamics, transmission of light in nonlinear optical materials, and wave dynamics in plasma media. The SDS system represents an extension of the standard Davey–Stewartson equations by introducing stochastic perturbations to discuss the dynamics of waves subjected to random influences. In order to analyze this model, we begin by decomposing the governing complex-valued equation into real and imaginary parts, obtaining a coupled system of nonlinear partial differential equations. The separation enables us to build an associated linear system whose solutions are polynomials parameterized with the physical constants of the model. Using a wave transformation and choosing suitable ansatz functions, we derive a class of exact stochastic optical soliton solutions by the Kumar-Malik method, which is a robust analytical approach well known for its competence in handling nonlinear structures. We give our solutions in various functional forms like trigonometric, hyperbolic, exponential, and Jacobi elliptic functions, and thus show the generality of the method. Furthermore, we provide a classification of these solutions into distinct categories such as bright solitons, dark solitons, singular and periodic structures, and noise-modulated waveforms. For the bright soliton solutions, we study the stability and dynamical behavior by conducting numerical simulations for different intensities of noise. The graphical representation of solutions in 3D, contour, and 2D plots contains rich dynamic features like amplitude modulation, deformation of wave profiles, and stochastic bifurcation onset. A comparative study with the existing literature is provided that emphasizes the novelty of the solutions presented and the universal utility of the stochastic DS framework to model real-world nonlinear systems. This work not only provides new exact solutions but also provides a deeper understanding of the effect of randomness on the propagation of solitons, making it a significant contribution to the analytic and physical knowledge of Stochastic partial differential equations in multidimensional models of waves.

1 Introduction

Stochastic partial differential equations (SPDEs) are mathematical models that can be used to explain the development of systems that exhibit randomness. These mathematical equations have been developed for numerous applications in a wide range of fields, such as engineering, finance, and physics, among others [1–3]. Deterministic models do not take into account the substantial influence of random factors on the system's behavior. As a result, the system's dynamics are more accurately and completely depicted. SPDE research has received a lot of interest because of its extensive application in a variety of fields, such as turbulence, climate modeling, financial engineering, materials technology, biology, and neurology [4–6]. During recent years, the use of analytical techniques in treating nonlinear evolution

✉ Karim K. Ahmed
karim.kamal.502@gmail.com

[1] Department of Information Security Technology, School of Applied Sciences, Cappadocia University, Nevsehir, Türkiye

[2] Department of Computer Engineering, Faculty of Engineering and Architecture, Istanbul Gelisim University, Istanbul, Türkiye

[3] Department of Mathematics, Faculty of Engineering, German International University (GIU), New Administrative Capital, Cairo, Egypt

Published online: 03 September 2025

equations has attracted increased attention as it has profound applications in actual phenomena such as oceanography, fluid dynamics, and plasma physics. For instance, Kumar and Rani [7] examined a (2+1)-dimensional dissipative long wave system, where they employed invariance analysis and optimal systems in order to obtain closed-form solutions that describe the dynamics of dissipative wave structures-vital for the description of energy loss in shallow water wave propagation. In another research work, the authors also explored the Boussinesq-Burgers model of relevance to ocean waves and derived various wave profiles and their significance in the depiction of the character of nonlinear and dispersive waves in viscous fluid media [8]. Besides, Rani and Kumar [9] examined the Jaulent–Miodek and Zakharov–Kuznetsov equations with a higher-order generalized method to expose the evolution and interaction of soliton solutions that are of crucial importance in describing nonlinear wave patterns in atmospheric and marine systems. Such investigations demonstrate the applicative relevance of analytical methods in describing multifaceted wave behavior in such a manner as to enable them to serve as effective tools for modeling and predicting natural phenomena in applied science.

Analyzing the SPDEs both analytically and numerically is one of their main difficulties. Numerous scholars have been working on SPDEs recently in an effort to find both approximate and exact solutions, including Li and Liu made investigations for the perturbed stochastic nonlinear Schrödinger equation [10]. For the modified Korteweg-de Vries equation with stochastic terms, Mohammed and Askar obtained some new analytical solutions [11]. Luo's research found new stochastic solutions to the fractional stochastic Kraenkel-Manna-Merle equation in ferromagnetic materials [12].

The retrieval of solitary wave solutions for nonlinear dynamical systems has become very important due to its applications in various disciplines. Soliton waves, a fascinating class of nonlinear wave solutions, maintain their structure and energy as they propagate through a medium. These solitary waves, also referred to as solitons, are commonly utilized in multiple fields. Their unique properties have made them a subject of intense study, particularly in relation to their response to noise. Understanding this behavior is crucial, as solitary waves play a key role in nonlinear dynamics. Investigating the interactions of these waves and their reactions to disturbances is essential for comprehending the overall system behavior. Nonlinear systems can show a range of responses to external perturbations or noise. The remarkable ability of solitary wave solutions to preserve their form and energy, despite such disturbances, highlights their significance in the presence of noise. To effectively utilize solitary waves in real-world applications and deepen our understanding of complex systems, it is crucial to investigate how they interact within noisy environments. To obtain solutions to mathematical models, many scientists have developed different methods. Some of them are the improved Adomian decomposition method [13], the modified extended direct algebraic method [14], the new mapping method [15], the extended F-expansion method [16, 17], the Riccati–Bernoulli sub-ODE method [18, 19], improved $\tan(\frac{\Phi(\xi)}{2})$-expansion method [20], and the $(\psi-\varphi)-$expansion method [21], the generalized $\left(\frac{G'}{G}\right)$ -expansion approach [22, 23].

Recent research has extensively investigated nonlinear wave equations using a variety of analytical approaches to construct soliton solutions and study their behavior. Rahman et al. studied the Westervelt equation's soliton solutions and dynamics using Matlab Symbolic Math Toolbox and Maple software, resulting in complex wave interactions suitable for acoustic modeling [24]. Arafat et al. explained wave profiles of (2+1)-dimensional Konopelchenko–Dubrovsky model by promoting mathematical physics using exact solutions [25]. Dey et al. explained soliton dynamics for a (3+1)-dimensional shallow water-like equation using the $(\phi'/\phi, 1/\phi)-$expansion method and provided insight into hydrodynamic systems [26]. Islam et al. analyzed the effect of stretch coordinates and conducted bifurcation and stability analysis of the Hamiltonian amplitude equation, enriching nonlinear stability theory phenomena [27]. Arafat et al. studied the mKdV-ZK model and unveiled rich soliton wave profiles and bifurcation structures [28]. Yiasir et al. also studied traveling wave solutions of the Boiti-Leon-Manna-Pempinelli equation, enriching the theoretical study of (2+1)-dimensional systems [29].

In addition, Arafat and Islam studied bifurcation and soliton solutions of the truncated M-fractional Kuralay-II equation [30], and Islam studied elastic inhomogeneous media solitons for doubly dispersive Murnaghan's rod model [31]. Islam also studied long wave-short wave resonance interaction equation soliton dynamics with nonlinear resonance phenomena [32]. Rayhanul Islam et al. showed novel results on stochastic chiral nonlinear Schrödinger equations, e.g., stability analysis of optical solitons [33]. Islam generalized to nano-ionic current equations and paraxial nonlinear Schrödinger models and demonstrated exact solutions and bifurcation analysis [34, 35].

Concurrently, Khan et al. studied the Shynaray-IIa equation and demonstrated soliton propagation dynamics [36]. They also investigated solitary solutions of the improved mKdV equation using advanced schemes [37]. Khan et al. have also found bifurcation and chaotic oscillations of the Kuralay-II equation with the use of conformable derivatives

and Jacobi elliptic expansions [38], and Farooq et al. have provided exact solutions of the same equation with M-fractional derivatives [39]. Collectively, these studies considerably advance the theoretical and computational position of soliton dynamics for high-dimensional nonlinear systems to new heights. The Davey–Stewartson equation (DSE), introduced by Davey and Stewartson in 1974, provides a framework for examining the time evolution of a three-dimensional wave packet in shallow water. It comprises a set of interrelated partial differential equations for the real field (mean flow) and the complex field (wave amplitude) [40]. The Davey–Stewartson (DS) system, originally derived to simulate the development of weakly nonlinear wave packets on water surfaces, has been further developed and applied in many fields of physics, including fluid dynamics, plasma physics, and nonlinear optics. The classic DS equations have been renowned for their capability to simulate multi-dimensional wave interactions, especially the modulation and stability of two-dimensional wave packets. To better capture more realistic real-world phenomena with uncertainty and environmental variations, the model is extended further to incorporate stochastic perturbations to yield stochastic Davey–Stewartson (SDS) equations. These stochastic extensions cover random effects like turbulent media, thermal noise, or external forcing, which are critical in real systems like optical fibers and Bose-Einstein condensates. Many studies have investigated the deterministic DS system through analytical and numerical methods; its stochastic counterparts, however, are fairly less investigated. The primary purpose of this study is to examine the stochastic Davey–Stewartson mathematical model (SDSMM) [41]:

$$i\Gamma_t + \frac{1}{2}a^2\left(\Gamma_{xx} + a^2\Gamma_{yy}\right) + \zeta\left|\Gamma\right|^2\Gamma - \Lambda_x\Gamma + iv\Gamma W_t = 0, \tag{1.1}$$

$$\Lambda_{xx} - a^2\Lambda_{yy} - 2\zeta\left(\left|\Lambda\right|^2\right)_x = 0, \tag{1.2}$$

in which $W = \pm 1$ and $a^2 = \pm 1$. For the cubic nonlinearity, the constant ζ is used. We are taking into account multiplicative noise, which is managed via the Borel function v and W_t is Brownian motion. There are two cases for the SDSM model. When $a = 1$, the equation is DSE-I; when $a = i$, it is DSE-II. The higher-dimensional equations, DSE-I and DSE-II, are integrable extensions of the nonlinear Schrödinger equation, and they have multiple applications, including the modeling of gravity-capillarity surface wave packets in shallow water. The SDS equation describes the evolution of weakly nonlinear, dispersive wave packets in a two-dimensional medium, often in the context of shallow water waves, plasma waves, or nonlinear optics, taking into account random fluctuations or noise present in realistic contexts. Applications of the solutions to the SDSMM include hydrodynamics, nonlinear optics, and plasma physics. For example, why microwaves and spatio-temporal optics work so well together can be explained by the outcomes of the SDSMMs.

Many researchers have used a variety of methodologies to study this model over the past few decades, some of which include the following: Askar et al. obtained different types of soliton solutions using the mapping method [42]. Using the $\left(\frac{G'}{G^2}\right)$-approximation, Tarıq et al. achieved kink, periodic, and rational solutions for the SDSM model [43]. In their study, Qi et al. used the improved modified extended tanh function method to gain new stochastic solutions [44].

1.1 Motivation of the Study

The primary goal of the current study is to solve the SDSM model using the Kumar-Malik method. We utilize this method, which yields four families of solutions. The Kumar-Malik method is a reliable approach to derive exact solutions for nonlinear systems. This method yields various types of soliton solutions, including bright, dark, and periodic wave solutions. Consequently, it is considered more efficient than other approaches, providing more accurate results. One limitation of this study is that the Kumar-Malik method is only applicable to certain types of ODEs. Furthermore, these outcomes are especially helpful for studying the SDSM model at the micro level since they provide information about how the nonlinear system responds to noise. In the case of zero noise strength, these solutions are equivalent to traditional soliton solutions. The bifurcation analysis has been applied to this model in [45].

This paper is divided into the following sections: An introduction to the SDSM model is given in Sect. 1. Section 2 describes the Wiener process. The basic principles of the Kumar-Malik method are described in Sect. 3. The given method is applied in Sect. 4. The graphical representation of some solutions is discussed in Sect. 5. Some comparisons with other research papers from the literature are presented in Sect. 6 . The results of the study are presented in Sect. 7.

2 Description of the Wiener Process

Take into consideration a non-differentiable Wiener process $W(t)$ with the next properties [41]:

$$\lim_{\delta t\to 0}\delta W_t = 0,$$
$$\lim_{\delta t\to 0}\frac{[\delta W_t]^M}{\delta t} = \begin{cases} 1, & M=2 \\ 0, & M=3,4,\ldots \end{cases}$$

Definition 1 When the subsequent conditions are satisfied, a motion is considered to be Brownian for the stochastic process $[W_t]_{t\le 0}$:

(1). When $t \le 0, W_t$ is the continues function.
(2). When $t_1 < t_2, W_{t_2} - W_{t_1}$ is independent.
(3). $W_{t_2} - W_{t_1}$ has a normal distribution $k(0, t_2 - t_1)$.
(4). $W_0 = 0$.

In this case, the Wiener process $W(t)$ time derivative is written as $W_t = \frac{dW}{dt}$.

3 Kumar-Malik Approach

3.1 Formulation of the Proposed Method

The Kumar-Malik approach is briefly described in this section [46].

Phase (1). Let us consider the following NLPDE:

$$\wp_1(\Gamma, \Gamma_x, \Gamma_y, \Gamma_t, \Gamma_{xx}, \ldots) = 0, \tag{3.1}$$

in which $\Gamma = \Gamma(x, y, t)$ is a polynomial function.

By applying the following wave transformation,

$$\begin{aligned}\Gamma(x,y,t) =& \ell(\xi)\times\exp^{\eta}, \qquad \xi = \rho_1 x + \rho_2 y - \rho_3 t,\\ & \eta = i\varpi - vW(t) - v^2 t,\end{aligned} \tag{3.2}$$

$$\begin{aligned}\Lambda(x,y,t) =& \hbar(\varpi)\times\exp^{\kappa}, \qquad \varpi = k_1 x + k_2 y + k_3 t,\\ & \kappa = -2vW(t) - 2v^2 t,\end{aligned} \tag{3.3}$$

Equation(3.1) is reduced as

$$\wp_2\left(\ell, \ell', \ell'', \ldots\right) = 0. \tag{3.4}$$

At this stage, all constants of integration are taken to be zero, and the reached ODE should be integrated as far as possible. In Eqs.(3.2)-(3.3), ρ_l and k_l $(l = 1, 2, 3)$ are constants.

Let the following solution form satisfies the Eq.(3.4):

$$\ell(\xi) = \Upsilon_0 + \sum_{j=1}^{n}\Upsilon_j \Theta(\xi)^j, \ \Upsilon_n \neq 0. \tag{3.5}$$

Here, Υ_j $(j = 1, 2, 3, \ldots, n)$ are undefined constants and the function $\Theta(\xi)$ fulfills the first-order ODE:

$$\begin{aligned}&[\Theta'(\xi)]^2\\ &= \left[\kappa_1\Theta(\xi)^4 + \kappa_2\Theta(\xi)^3 + \kappa_3\Theta(\xi)^2 + \kappa_4\Theta(\xi) + \kappa_5\right]\\ &, \ \kappa_1 \neq 0,\end{aligned} \tag{3.6}$$

where κ_j $(j = 1, 2, \ldots, 5)$ are real constants.

Phase (2). The balancing rule is used to find the value of n in Eq.(3.5).

Phase (3). By substituting Eq.(3.5) and its derivatives with Eq.(3.6) into Eq.(3.4), a polynomial in $\Theta(\xi)\Theta'(\xi)$ is obtained. By collecting the coefficients of the various powers and setting them to zero, we obtain an algebraic system of equations involving the unknown parameters k_2, Υ_j $(j = 1, 2, \ldots, n)$, and κ_j $(j = 1, 2, \ldots, 5)$. The soliton solutions for Eq.(3.4) are found by solving this system.

Phase (4). From the solutions of EqS.(3.4) and (3.2), several analytical solutions to the Eq.(3.1) are derived.

The Eq.(3.6) solution is given below:

Condition (1). Assuming $\kappa_4 = \frac{\kappa_2\left(4\kappa_1\kappa_3 - \kappa_2^2\right)}{8\kappa_1^2}$, $\kappa_5 = 0$, the Jacobi elliptic solutions take the following form:

Sub-condition (1.1). When $\kappa_1 < 0$, and $(4\kappa_1\kappa_3 - \kappa_2^2) > 0$, then

$$\Theta_1(\xi) = -\frac{\kappa_2}{4\kappa_1} + \frac{\kappa_2}{4\kappa_1}\mathrm{cn}\left[\frac{\sqrt{-\kappa_1(4\kappa_1\kappa_3 - \kappa_2^2)}\xi}{2\kappa_1}, \frac{\kappa_2}{2\sqrt{(4\kappa_1\kappa_3 - \kappa_2^2)}}\right], \tag{3.7}$$

$$\Theta_2(\xi) = -\frac{\kappa_2}{4\kappa_1} + \frac{\kappa_2}{4\kappa_1}\mathrm{dn}\left[\frac{\kappa_2\xi}{4\sqrt{-\kappa_1}}, \frac{2\sqrt{(4\kappa_1\kappa_3 - \kappa_2^2)}}{\kappa_2}\right]. \tag{3.8}$$

Sub-condition (1.2). When $\kappa_1 < 0$, $(4\kappa_1\kappa_3 - \kappa_2^2) < 0$, and $(16\kappa_1\kappa_3 - 5\kappa_2^2) < 0$, then

$$\Theta_3(\xi) = -\frac{\kappa_2}{4\kappa_1} + \frac{\sqrt{-(16\kappa_1\kappa_3 - 5\kappa_2^2)}}{4\kappa_1}\mathrm{cn}\left[\frac{\sqrt{(4\kappa_1\kappa_3 - \kappa_2^2)\kappa_1}\xi}{2\kappa_1}, \frac{2\sqrt{(4\kappa_1\kappa_3 - \kappa_2^2)(16\kappa_1\kappa_3 - 5\kappa_2^2)}}{2(4\kappa_1\kappa_3 - \kappa_2^2)}\right], \tag{3.9}$$

$$\Theta_4(\xi) = -\frac{\kappa_2}{4\kappa_1} + \frac{\sqrt{-(16\kappa_1\kappa_3 - 5\kappa_2^2)}}{4\kappa_1}\mathrm{dn}\left[\frac{\sqrt{(4\kappa_1\kappa_3 - \kappa_2^2)\kappa_2}\xi}{4\kappa_1}, \frac{2\sqrt{(4\kappa_1\kappa_3 - \kappa_2^2)(16\kappa_1\kappa_3 - 5\kappa_2^2)}}{(16\kappa_1\kappa_3 - 5\kappa_2^2)}\right]. \tag{3.10}$$

Sub-condition (1.3). When $\kappa_1 < 0$, $(4\kappa_1\kappa_3 - \kappa_2^2) > 0$, and $(16\kappa_1\kappa_3 - 5\kappa_2^2) < 0$, then

$$\Theta_5(\xi) = -\frac{\kappa_2}{4\kappa_1} + \frac{\sqrt{-(16\kappa_1\kappa_3 - 5\kappa_2^2)}}{4\kappa_1}\mathrm{nc}\left[\frac{\sqrt{-(4\kappa_1\kappa_3 - \kappa_2^2)\kappa_1}\xi}{2\kappa_1}, \frac{\kappa_2}{2\sqrt{(4\kappa_1\kappa_3 - \kappa_2^2)}}\right], \tag{3.11}$$

$$\Theta_6(\xi) = -\frac{\kappa_2}{4\kappa_1} + \frac{\sqrt{-(16\kappa_1\kappa_3 - 5\kappa_2^2)}}{4\kappa_1}\mathrm{nd}\left[\frac{\kappa_2\xi}{4\sqrt{-\kappa_1}}, \frac{2\sqrt{(4\kappa_1\kappa_3 - \kappa_2^2)}}{\kappa_2}\right]. \tag{3.12}$$

Sub-condition (1.4). When $\kappa_1(4\kappa_1\kappa_3 - \kappa_2^2) > 0$, and $(4\kappa_1\kappa_3 - \kappa_2^2)(16\kappa_1\kappa_3 - 5\kappa_2^2) > 0$, then

$$\Theta_7(\xi) = -\frac{\kappa_2}{4\kappa_1} + \frac{(16\kappa_1\kappa_3 - 5\kappa_2^2)}{4\kappa_1}\ \mathrm{nc}\left[\frac{\sqrt{\kappa_1(4\kappa_1\kappa_3 - \kappa_2^2)}\xi}{2\kappa_1}, \frac{\sqrt{(4\kappa_1\kappa_3 - \kappa_2^2)(16\kappa_1\kappa_3 - 5\kappa_2^2)}}{\kappa_1}\right], \tag{3.13}$$

$$\Theta_8(\xi) = -\frac{\kappa_2}{4\kappa_1} + \frac{(16\kappa_1\kappa_3 - 5\kappa_2^2)}{4\kappa_1}\ \mathrm{nd}\left[\frac{\sqrt{\kappa_1(16\kappa_1\kappa_3 - 5\kappa_2^2)}\xi}{4\kappa_1}, \frac{2\sqrt{(4\kappa_1\kappa_3 - \kappa_2^2)(16\kappa_1\kappa_3 - 5\kappa_2^2)}}{\kappa_2}\right]. \tag{3.14}$$

Sub-condition (1.5). When $\kappa_1 > 0$, and $(16\kappa_1\kappa_3 - 5\kappa_2^2) < 0$, then

$$\Theta_9(\xi) = -\frac{\kappa_2}{4\kappa_1} + \frac{(16\kappa_1\kappa_3 - 5\kappa_2^2)}{4\kappa_1}\ \mathrm{ns}\left[\frac{\kappa_2\xi}{4\sqrt{\kappa_1}}, \frac{\sqrt{-(16\kappa_1\kappa_3 - 5\kappa_2^2)}}{\kappa_2}\right], \tag{3.15}$$

$$\Theta_{10}(\xi) = -\frac{\kappa_2}{4\kappa_1} + \frac{\sqrt{-(16\kappa_1\kappa_3 - 5\kappa_2^2)}}{4\kappa_1}\mathrm{ns}\left[\frac{\sqrt{-\kappa_1(16\kappa_1\kappa_3 - 5\kappa_2^2)}\xi}{4\kappa_1}, \frac{\kappa_2}{\sqrt{-(16\kappa_1\kappa_3 - 5\kappa_2^2)}}\right], \tag{3.16}$$

$$\Theta_{11}(\xi) = -\frac{\kappa_2}{4\kappa_1} + \frac{\sqrt{-(16\kappa_1\kappa_3 - 5\kappa_2^2)}}{4\kappa_1}\mathrm{sn}\left[\frac{\kappa_2\xi}{4\sqrt{\kappa_1}}, \frac{\sqrt{-(16\kappa_1\kappa_3 - 5\kappa_2^2)}}{\kappa_2}\right], \tag{3.17}$$

$$\Theta_{12}(\xi) = -\frac{\kappa_2}{4\kappa_1} + \frac{(16\kappa_1\kappa_3 - 5\kappa_2^2)}{4\kappa_1}\mathrm{sn}\left[\frac{\sqrt{-\kappa_1(16\kappa_1\kappa_3 - 5\kappa_2^2)}\xi}{4\kappa_1}, \frac{\kappa_2}{\sqrt{-(16\kappa_1\kappa_3 - 5\kappa_2^2)}}\right]. \tag{3.18}$$

Remark 3.1 In this context, the elliptic modulus is represented by the second term in the Jacobi elliptic functions, where *m* stands as the modulus in $sn[\xi, m]$.

Condition (2). Assuming $\kappa_4 = \frac{\kappa_2(4\kappa_1\kappa_3 - \kappa_2^2)}{8\kappa_1^2}$, $\kappa_5 = \frac{(4\kappa_1\kappa_3 - \kappa_2^2)^2}{64\kappa_1^3}$, the solutions for the trigonometric and hyperbolic functions are shown below:

Sub-condition (2.1). When $\kappa_1 > 0$, and $(8\kappa_1\kappa_3 - 3\kappa_2^2) < 0$, then

$$\Theta_{13}(\xi) = -\frac{\kappa_2}{4\kappa_1} + \frac{\sqrt{-(8\kappa_1\kappa_3 - 3\kappa_2^2)}}{4\kappa_1}\tanh\left[\frac{\sqrt{-\kappa_1(8\kappa_1\kappa_3 - 3\kappa_2^2)}\xi}{4\kappa_1}\right], \tag{3.19}$$

$$\Theta_{14}(\eta) = -\frac{\kappa_2}{4\kappa_1} + \frac{\sqrt{-(8\kappa_1\kappa_3 - 3\kappa_2^2)}}{4\kappa_1}\coth\left[\frac{\sqrt{-\kappa_1(8\kappa_1\kappa_3 - 3\kappa_2^2)}\xi}{4\kappa_1}\right]. \tag{3.20}$$

Sub-condition (2.2). When $\kappa_1 > 0$, and $(8\kappa_1\kappa_3 - 3\kappa_2^2) > 0$, then

$$\Theta_{15}(\xi) = -\frac{\kappa_2}{4\kappa_1} + \frac{\sqrt{(8\kappa_1\kappa_3 - 3\kappa_2^2)}}{4\kappa_1}\tan\left[\frac{\sqrt{\kappa_1(8\kappa_1\kappa_3 - 3\kappa_2^2)}\xi}{4\kappa_1}\right], \tag{3.21}$$

$$\Theta_{16}(\xi) = -\frac{\kappa_2}{4\kappa_1} + \frac{\sqrt{(8\kappa_1\kappa_3 - 3\kappa_2^2)}}{4\kappa_1}\cot\left[\frac{\sqrt{-\kappa_1(8\kappa_1\kappa_3 - 3\kappa_2^2)}\xi}{4\kappa_1}\right]. \tag{3.22}$$

Condition (3). Assuming $\kappa_4 = \frac{\kappa_2(4\kappa_1\kappa_3 - \kappa_2^2)}{8\kappa_1^2}$, and $\kappa_5 = \frac{\kappa_2^2(16\kappa_1\kappa_3 - 5\kappa_2^2)^2}{256\kappa_1^3}$, the hyperbolic and trigonometric solutions are given as follows:

Sub-condition (3.1). When $\kappa_1 < 0$, and $(8\kappa_1\kappa_3 - 3\kappa_2^2) < 0$, then

$$\Theta_{17}(\xi) = -\frac{\kappa_2}{4\kappa_1} + \frac{\sqrt{-2(8\kappa_1\kappa_3 - 3\kappa_2^2)}}{4\kappa_1}\mathrm{sech}\left[\frac{\sqrt{2\kappa_1(8\kappa_1\kappa_3 - 3\kappa_2^2)}\xi}{4\kappa_1}\right]. \tag{3.23}$$

Sub-condition (3.2). When $\kappa_1 > 0$, and $(8\kappa_1\kappa_3 - 3\kappa_2^2) > 0$, then

$$\Theta_{18}(\xi) = -\frac{\kappa_2}{4\kappa_1} + \frac{\sqrt{2(8\kappa_1\kappa_3 - 3\kappa_2^2)}}{4\kappa_1}\ \mathrm{csch}\left[\frac{\sqrt{2\kappa_1(8\kappa_1\kappa_3 - 3\kappa_2^2)}\xi}{4\kappa_1}\right]. \tag{3.24}$$

Sub-condition (3.3). When $\kappa_1 > 0$, and $(8\kappa_1\kappa_3 - 3\kappa_2^2) < 0$, then

$$\Theta_{19}(\xi) = -\frac{\kappa_2}{4\kappa_1} + \frac{\sqrt{-2(8\kappa_1\kappa_3 - 3\kappa_2^2)}\sec\left[\frac{\sqrt{-2\kappa_1(8\kappa_1\kappa_3-3\kappa_2^2)}\xi}{4\kappa_1}\right]}{4\kappa_1}, \tag{3.25}$$

$$\Theta_{20}(\xi) = -\frac{\kappa_2}{4\kappa_1} + \frac{\sqrt{-2(8\kappa_1\kappa_3 - 3\kappa_2^2)}\csc\left[\frac{\sqrt{-2\kappa_1(8\kappa_1\kappa_3-3\kappa_2^2)}\xi}{4\kappa_1}\right]}{4\kappa_1}. \tag{3.26}$$

Condition (4). Assuming $\kappa_2 = 0$, $\kappa_4 = 0$, $\kappa_5 = 0$, $\kappa_3 > 0$, the exponential solutions are expressed as:

$$\Theta_{21}(\xi) = \frac{4\varrho\kappa_3}{4\varrho^2\exp\left[\sqrt{\kappa_3}\xi\right] - \kappa_1\kappa_3\exp\left[-\sqrt{\kappa_3}\xi\right]}. \tag{3.27}$$

Sub-condition (4.1). If $\kappa_1 = -\frac{4\varrho^2}{\kappa_3}$, Eq.(3.27) simplifies to:

$$\Theta_{22}(\xi) = \frac{\kappa_3}{2\varrho}\ \mathrm{sech}\left[-\sqrt{\kappa_3}\xi\right]. \tag{3.28}$$

Sub-condition (4.2). If $\kappa_1 = \frac{4\varrho^2}{\kappa_3}$, Eq.(3.27) simplifies to:

$$\Theta_{23}(\xi) = \frac{\kappa_3}{2\varrho}\ \mathrm{csch}\left[-\sqrt{\kappa_3}\xi\right]. \tag{3.29}$$

3.2 Novelty of the Method

In contrast to other classical methods such as Hirota's bilinear approach [47], Lie symmetry analysis [48], and the Darboux transformation [49], the Kumar-Malik method demonstrates a greater capacity for generating diversified and complicated solution profiles. For instance, whereas Hirota's technique tends to generate multi-soliton solutions in bilinear form, it becomes algebraically cumbersome and less effective when stochastic perturbations or variable coefficients are involved. The Lie symmetry approach, though systematic and geometrically insightful, has a tendency to lead to similarity reductions rather than necessarily producing closed-form solutions for higher dimensions. Similarly, the Darboux transformation is powerful for integrable systems but is only generally applicable to rational or exponential soliton solutions.

For comparison, the Kumar-Malik approach, when applied to the stochastic Davey–Stewartson (SDS) model, sufficiently generates a wide range of exact solutions like bright, dark, singular, breather, periodic, Jacobi elliptic, and exponential ones with one general framework. Above all, it can handle the presence of the random effects as noise terms, allowing one to model wave behaviors more realistically. The approach also embodies the bifurcation among various dynamical behaviors (e.g., collision, bifurcation) through controllable parameters, which are harder to explore with conventional methods. Hence, from the viewpoint of solution diversity, adaptability to stochasticity, and physical interpretability, the Kumar-Malik method enjoys an unparalleled advantage in handling nonlinear, noise-driven, multi-dimensional wave equations.

4 Extraction of Soliton Solutions

By implementing Eq.(3.2), the real and imaginary components of Eq.(1.1) can be achieved as follows:

$$\left(\frac{1}{2}\rho_1^2a^2 + \frac{1}{2}\rho_2^2a^4\right)\ell'' - \left(k_3 + \frac{1}{2}\rho_1^2k_1^2 + \frac{1}{2}\rho_2^2a^4\right)\ell + \left(\zeta\ell^3 - \rho_1\ell\hbar'\right)e^{\left[-vW(t)-v^2t\right]} = 0, \tag{4.1}$$

$$\left(\rho_1^2 - \rho_2^2a^2\right)\hbar'' - 2\rho_1\zeta\left(\ell^2\right)' = 0, \tag{4.2}$$

and

$$\left(-\rho_3 + 2\rho_2k_1 + 2\rho_2k_2\right)\ell' = 0. \tag{4.3}$$

From Eq.(4.3), the constraint condition is derived as:

$$\rho_3 = 2\rho_2k_1 + 2\rho_2k_2. \tag{4.4}$$

After integrating Eq.(4.2) once and setting the integrating constants to zero, we obtain

$$\hbar' = \frac{2\rho_1\zeta}{(\rho_1^2 - \rho_2^2 a^2)}\left(\ell^2\right). \tag{4.5}$$

Inserting Eq.(4.5) into Eq.(4.1) gives us:

$$\begin{aligned}\ell'' - \frac{\left(2k_3 + k_1^2a^2 + k_2^2a^4\right)}{a^2\left(\rho_1^2 + \rho_2^2a^2\right)}\ell \\ + \left(\frac{2\zeta}{a^2\left(\rho_1^2 - \rho_2^2a^2\right)}\right)\ell^3 e^{\left[-vW(t) - v^2t\right]} = 0.\end{aligned} \tag{4.6}$$

Taking the expectation of $\mathbb{E}$ on Eq. (12) gives us:

$$\begin{aligned}\ell'' - \frac{\left(2k_3 + k_1^2a^2 + k_2^2a^4\right)}{a^2\left(\rho_1^2 + \rho_2^2a^2\right)}\ell \\ + \left(\frac{2\zeta}{a^2\left(\rho_1^2 - \rho_2^2a^2\right)}\right)\ell^3\mathbb{E}\left[e^{(-vW(t))}\right] = 0,\end{aligned} \tag{4.7}$$

in which Wiener process is represented by $W(t)$, thus $\mathbb{E}\left[e^{(-vW(t))}\right] = e^{(v^2t)}$. Therefore, Eq.(4.7) turns into:

$$\begin{aligned}\ell'' - \frac{\left(2k_3 + k_1^2a^2 + k_2^2a^4\right)}{a^2\left(\rho_1^2 + \rho_2^2a^2\right)}\ell \\ + \left(\frac{2\zeta}{a^2\left(\rho_1^2 - \rho_2^2a^2\right)}\right)\ell^3 = 0.\end{aligned} \tag{4.8}$$

From applying the balancing rule to Eq.(4.8), we obtain $n = 1$. Hence, Eq.(3.5) becomes

$$\ell(\xi) = \Upsilon_0 + \Upsilon_1\Theta\left(\xi\right). \tag{4.9}$$

By applying the phases of the method, we get the following Cluster for **Conditions (1)-(3)**.

Cluster:

$$\begin{aligned}k_2 = \frac{1}{4a^2} \\ \sqrt{\frac{16\kappa_1\left(\kappa_3\rho_2^2a^4 + \left(\kappa_3\rho_1^2 - k_1^2\right)a^2 - 2k_3\right) - 6a^2\kappa_2^2\left(a^2\rho_2^2 + \rho_1^2\right)}{\kappa_1}},\end{aligned}$$

$$\begin{aligned}\Upsilon_0 = \frac{a\kappa_2}{4}\sqrt{-\frac{-a^2\rho_2^2 + \rho_1^2}{\zeta\kappa_1}}, \quad \Upsilon_1 \\ = a\kappa_1\sqrt{-\frac{-a^2\rho_2^2 + \rho_1^2}{\zeta\kappa_1}}.\end{aligned} \tag{4.10}$$

If the phases of the method are applied:

Condition (1). When $\kappa_4 = \frac{\kappa_2\left(4\kappa_1\kappa_3 - \kappa_2^2\right)}{8\kappa_1^2}$, $\kappa_5 = 0$, then we have Jacobi elliptic solutions as:

Inserting Eq.(4.10) into Eq.(4.9) gives the comprehensive solutions to Eq.(1.1):

Sub-condition (1.1). For $\kappa_1 < 0$, and $\left(4\kappa_1\kappa_3 - \kappa_2^2\right) > 0$, then we get

$$\begin{aligned}\Gamma_1\left(x, y, t\right) \\ = \left\{\begin{array}{c} \frac{a\kappa_2}{4}\sqrt{\frac{(a\rho_2 - \rho_1)(a\rho_2 + \rho_1)}{\zeta\kappa_1}} \\ \times cn\left(\frac{\sqrt{-\left(4\kappa_1\kappa_3 - \kappa_2^2\right)\kappa_1}}{2\kappa_1}\left(\rho_1x + \rho_2y - \rho_3t\right), \frac{\kappa_2}{2\sqrt{\left(4\kappa_1\kappa_3 - \kappa_2^2\right)}}\right)\end{array}\right\} \\ \times \exp\left[-vW\left(t\right) - v^2t + i\left(k_1x + k_2y + k_3t\right)\right],\end{aligned} \tag{4.11}$$

$$\begin{aligned}\Lambda_1\left(x, y, t\right) \\ = \left\{\begin{array}{c} \left(\begin{array}{c} E\left(\mathrm{sn}\left(\frac{\sqrt{-\kappa_1\left(4\kappa_1\kappa_3 - \kappa_2^2\right)}\left(k_3t + k_1x + k_2y\right)}{2\kappa_1}, \frac{\kappa_2}{2\sqrt{4\kappa_1\kappa_3 - \kappa_2^2}}\right), \frac{\kappa_2}{2\sqrt{4\kappa_1\kappa_3 - \kappa_2^2}}\right) \\ -\frac{\left(1 - \frac{\kappa_2^2}{16\kappa_1\kappa_3 - 4\kappa_2^2}\right)\sqrt{-\kappa_1\left(4\kappa_1\kappa_3 - \kappa_2^2\right)}\left(k_3t + k_1x + k_2y\right)}{2\kappa_1} \\ \times\frac{\rho_1(a\rho_2 - \rho_1)(a\rho_2 + \rho_1)a\left(4\kappa_1\kappa_3 - \kappa_2^2\right)^2}{\left(-a^2\rho_2^2 + \rho_1^2\right)\sqrt{-\kappa_1\left(4\kappa_1\kappa_3 - \kappa_2^2\right)}} \\ \times\exp\left[-2vW\left(t\right) - 2v^2t\right]\end{array}\right)\end{array}\right\},\end{aligned} \tag{4.12}$$

$$\Gamma_2(x,y,t) = \left\{ \begin{array}{c} \frac{a\kappa_2}{4}\sqrt{\frac{(a\rho_2-\rho_1)(a\rho_2+\rho_1)}{\zeta\kappa_1}} \\ \times dn\left(\frac{\kappa_2}{4\sqrt{-\kappa_1}}(\rho_1 x+\rho_2 y-\rho_3 t), \frac{2\sqrt{\left(4\kappa_1\kappa_3-\kappa_2^2\right)}}{\kappa_2}\right) \end{array} \right\} \quad (4.13)$$
$$\times \exp\left[-vW(t)-v^2t+i(k_1x+k_2y+k_3t)\right],$$

$$\Lambda_2(x,y,t) = \left\{ \begin{array}{c} E\left(\mathrm{sn}\left(\frac{\kappa_2(k_3t+xk_1+yk_2)}{4\sqrt{-\kappa_1}}, \frac{2\sqrt{4\kappa_1\kappa_3-\kappa_2^2}}{\kappa_2}\right), \frac{2\sqrt{4\kappa_1\kappa_3-\kappa_2^2}}{\kappa_2}\right) \\ \times \frac{\rho_1(a\rho_2-\rho_1)(a\rho_2+\rho_1)a^2\kappa_2\sqrt{-\kappa_1}}{2\left(-a^2\rho_2^2+\rho_1^2\right)\kappa_1} \\ \times \exp\left[-2vW(t)-2v^2t\right] \end{array} \right\}. \quad (4.14)$$

Sub-condition (1.2). For $\kappa_1<0, \quad (4\kappa_1\kappa_3-\kappa_2^2)<0$, and $(16\kappa_1\kappa_3-5\kappa_2^2)<0$, then we reach

$$\Gamma_3(x,y,t) = \left\{ \begin{array}{c} \frac{a\sqrt{(-16\kappa_1\kappa_3+5\kappa_2^2)}}{4}\sqrt{\frac{(a\rho_2-\rho_1)(a\rho_2+\rho_1)}{\zeta\kappa_1}} \\ \times cn\left(\frac{\sqrt{\left(4\kappa_1\kappa_3-\kappa_2^2\right)\kappa_1}}{2\kappa_1}(\rho_1 x+\rho_2 y-\rho_3 t), \frac{\sqrt{\left(4\kappa_1\kappa_3-\kappa_2^2\right)(16\kappa_1\kappa_3-5\kappa_2^2)}}{2\left(4\kappa_1\kappa_3-\kappa_2^2\right)}\right) \end{array} \right\}$$
$$\times \exp\left[-vW(t)-v^2t+i(k_1x+k_2y+k_3t)\right], \quad (4.15)$$

$$\Lambda_3(x,y,t) = \left\{ \left(\begin{array}{c} E\left(\mathrm{sn}\left(\frac{\sqrt{\kappa_1\left(4\kappa_1\kappa_3-\kappa_2^2\right)}(tk_3+xk_1+yk_2)}{2\kappa_1}, \frac{\sqrt{16\kappa_1\kappa_3-5\kappa_2^2}}{2\sqrt{4\kappa_1\kappa_3-\kappa_2^2}}\right), \frac{\sqrt{16\kappa_1\kappa_3-5\kappa_2^2}}{2\sqrt{4\kappa_1\kappa_3-\kappa_2^2}}\right) \\ -\frac{\left(1-\frac{16\kappa_1\kappa_3-5\kappa_2^2}{16\kappa_1\kappa_3-4\kappa_2^2}\right)\sqrt{\kappa_1\left(4\kappa_1\kappa_3-\kappa_2^2\right)}(tk_3+xk_1+yk_2)}{2\kappa_1} \\ \times \frac{\rho_1(a\rho_2-\rho_1)(a\rho_2+\rho_1)a^2\left((-16\kappa_1\kappa_3+5\kappa_2)\left(4\kappa_1\kappa_3-\kappa_2^2\right)^2\right)}{\left(-a^2\rho_2^2+\rho_1^2\right)\left(16\kappa_1\kappa_3-5\kappa_2^2\right)\sqrt{\kappa_1\left(4\kappa_1\kappa_3-\kappa_2^2\right)}} \\ \times \exp\left[-2vW(t)-2v^2t\right] \end{array} \right) \right\}, \quad (4.16)$$

$$\Gamma_4(x,y,t) = \left\{ \begin{array}{c} \frac{a\sqrt{(-16\kappa_1\kappa_3+5\kappa_2^2)}}{4}\sqrt{\frac{(a\rho_2-\rho_1)(a\rho_2+\rho_1)}{\zeta\kappa_1}} \\ \times dn\left(\frac{\sqrt{(16\kappa_1\kappa_3-5\kappa_2^2)\kappa_1}}{4\kappa_1}(\rho_1 x+\rho_2 y-\rho_3 t), \frac{2\sqrt{\left(4\kappa_1\kappa_3-\kappa_2^2\right)(16\kappa_1\kappa_3-5\kappa_2^2)}}{(16\kappa_1\kappa_3-5\kappa_2^2)}\right) \end{array} \right\}$$
$$\times \exp\left[-vW(t)-v^2t+i(k_1x+k_2y+k_3t)\right], \quad (4.17)$$

$$\Lambda_4(x,y,t) = \left\{ \begin{array}{c} E\left(\mathrm{sn}\left(\frac{\sqrt{\kappa_1\left(16\kappa_1\kappa_3-5\kappa_2^2\right)}(tk_3+xk_1+yk_2)}{4\kappa_1}, \frac{2\sqrt{4\kappa_1\kappa_3-\kappa_2^2}}{\sqrt{16\kappa_1\kappa_3-5\kappa_2^2}}\right), \frac{2\sqrt{4\kappa_1\kappa_3-\kappa_2^2}}{\sqrt{16\kappa_1\kappa_3-5\kappa_2^2}}\right) \\ \times \frac{\rho_1(a\rho_2-\rho_1)(a\rho_2+\rho_1)a^2\left(-16\kappa_1\kappa_3+5\kappa_2^2\right)}{2\left(-a^2\rho_2^2+\rho_1^2\right)\sqrt{\kappa_1\left(16\kappa_1\kappa_3-5\kappa_2^2\right)}} \\ \times \exp\left[-2vW(t)-2v^2t\right] \end{array} \right\}. \quad (4.18)$$

Sub-condition (1.3). For $\kappa_1<0, \quad (4\kappa_1\kappa_3-\kappa_2^2)>0$, and $(16\kappa_1\kappa_3-5\kappa_2^2)<0$, then we find

$$\Gamma_5(x,y,t) = \left\{ \begin{array}{c} \frac{a\sqrt{(-16\kappa_1\kappa_3+5\kappa_2^2)}}{4}\sqrt{\frac{(a\rho_2-\rho_1)(a\rho_2+\rho_1)}{\zeta\kappa_1}} \\ \times nc\left(\frac{\sqrt{-\left(4\kappa_1\kappa_3-\kappa_2^2\right)\kappa_1}}{2\kappa_1}(\rho_1 x+\rho_2 y-\rho_3 t), \frac{\kappa_2}{2\sqrt{\left(4\kappa_1\kappa_3-\kappa_2^2\right)}}\right) \end{array} \right\} \quad (4.19)$$
$$\times \exp\left[-vW(t)-v^2t+i(k_1x+k_2y+k_3t)\right],$$

$$\Lambda_5(x,y,t) = \left\{ \left(\begin{array}{c} \frac{\left(1-\frac{\kappa_2^2}{16\kappa_1\kappa_3-4\kappa_2^2}\right)\sqrt{-\kappa_1\left(4\kappa_1\kappa_3-\kappa_2^2\right)}\,(tk_3+xk_1+yk_2)}{2\kappa_1} \\ -E\left(\mathrm{sn}\left(\frac{\sqrt{-\kappa_1\left(4\kappa_1\kappa_3-\kappa_2^2\right)}\,(tk_3+xk_1+yk_2)}{2\kappa_1},\frac{\kappa_2}{2\sqrt{4\kappa_1\kappa_3-\kappa_2^2}}\right),\frac{\kappa_2}{2\sqrt{4\kappa_1\kappa_3-\kappa_2^2}}\right) \\ +\frac{\mathrm{dc}\left(\frac{\sqrt{-\kappa_1\left(4\kappa_1\kappa_3-\kappa_2^2\right)}\,(tk_3+xk_1+yk_2)}{2\kappa_1},\frac{\kappa_2}{2\sqrt{4\kappa_1\kappa_3-\kappa_2^2}}\right)\mathrm{sc}\left(\frac{\sqrt{-\kappa_1\left(4\kappa_1\kappa_3-\kappa_2^2\right)}\,(tk_3+xk_1+yk_2)}{2\kappa_1},\frac{\kappa_2}{2\sqrt{4\kappa_1\kappa_3-\kappa_2^2}}\right)}{\mathrm{nc}\left(\frac{\sqrt{-\kappa_1\left(4\kappa_1\kappa_3-\kappa_2^2\right)}\,(tk_3+xk_1+yk_2)}{2\kappa_1},\frac{\kappa_2}{2\sqrt{4\kappa_1\kappa_3-\kappa_2^2}}\right)} \\ \times\frac{\rho_1(a\rho_2-\rho_1)(a\rho_2+\rho_1)a^2\left(-16\kappa_1\kappa_3+5\kappa_2^2\right)}{4\left(-a^2\rho_2^2+\rho_1^2\right)\left(1-\frac{\kappa_2^2}{16\kappa_1\kappa_3-4\kappa_2^2}\right)\sqrt{-\kappa_1\left(4\kappa_1\kappa_3-\kappa_2^2\right)}} \\ \times\exp\left[-2vW(t)-2v^2t\right] \end{array} \right) \right\}, \tag{4.20}$$

$$\Gamma_6(x,y,t) = \left\{ \begin{array}{c} \frac{a\sqrt{\left(-16\kappa_1\kappa_3+5\kappa_2^2\right)}}{4}\sqrt{\frac{(a\rho_2-\rho_1)(a\rho_2+\rho_1)}{\zeta\kappa_1}} \\ \times nd\left(\frac{\kappa_2}{4\sqrt{-\kappa_1}}\left(\rho_1x+\rho_2y-\rho_3t\right),\frac{2\sqrt{\left(4\kappa_1\kappa_3-\kappa_2^2\right)}}{\kappa_2}\right) \end{array} \right\} \\ \times\exp\left[-vW(t)-v^2t+i\left(k_1x+k_2y+k_3t\right)\right]. \tag{4.21}$$

$$\Lambda_6(x,y,t) = \left\{ \left(\begin{array}{c} E\left(\mathrm{sn}\left(\frac{\kappa_2(k_3t+k_1x+k_2y)}{4\sqrt{-\kappa_1}},\frac{2\sqrt{4\kappa_1\kappa_3-\kappa_2^2}}{\kappa_2}\right),\frac{2\sqrt{4\kappa_1\kappa_3-\kappa_2^2}}{\kappa_2}\right) \\ -\frac{4\left(4\kappa_1\kappa_3-\kappa_2^2\right)\mathrm{sd}\left(\frac{\kappa_2(k_3t+k_1x+k_2y)}{4\sqrt{-\kappa_1}},\frac{2\sqrt{4\kappa_1\kappa_3-\kappa_2^2}}{\kappa_2}\right)\mathrm{cd}\left(\frac{\kappa_2(k_3t+k_1x+k_2y)}{4\sqrt{-\kappa_1}},\frac{2\sqrt{4\kappa_1\kappa_3-\kappa_2^2}}{\kappa_2}\right)}{\kappa_2^2\mathrm{nd}\left(\frac{\kappa_2(k_3t+k_1x+k_2y)}{4\sqrt{-\kappa_1}},\frac{2\sqrt{4\kappa_1\kappa_3-\kappa_2^2}}{\kappa_2}\right)} \\ \times\frac{\rho_1(a\rho_2-\rho_1)(a\rho_2+\rho_1)a^2\left(-16\kappa_1\kappa_3+5\kappa_2^2\right)\sqrt{-\kappa_1}}{2\left(-a^2\rho_2^2+\rho_1^2\right)\kappa_1\left(1-\frac{4\left(4\kappa_1\kappa_3-\kappa_2^2\right)}{\kappa_2^2}\right)\kappa_2} \\ \times\exp\left[-2vW(t)-2v^2t\right] \end{array} \right) \right\}, \tag{4.22}$$

Sub-condition (1.4). For $\kappa_1(4\kappa_1\kappa_3-\kappa_2^2)>0$, and $(4\kappa_1\kappa_3-\kappa_2^2)(16\kappa_1\kappa_3-5\kappa_2^2)>0$, then we get

$$\begin{aligned}&\Gamma_7(x,y,t)\\&=\left\{\begin{array}{c}\frac{a\kappa_2}{4}\sqrt{\frac{(a\rho_2-\rho_1)(a\rho_2+\rho_1)}{\zeta\kappa_1}}\\ \times nc\left(\frac{\sqrt{\left(4\kappa_1\kappa_3-\kappa_2^2\right)\kappa_1}}{2\kappa_1}(\rho_1x+\rho_2y-\rho_3t),\frac{\sqrt{\left(4\kappa_1\kappa_3-\kappa_2^2\right)\left(16\kappa_1\kappa_3-5\kappa_2^2\right)}}{2\left(4\kappa_1\kappa_3-\kappa_2^2\right)}\right)\end{array}\right\}\\&\times\exp\left[-vW(t)-v^2t+i(k_1x+k_2y+k_3t)\right],\end{aligned}\tag{4.23}$$

$$\begin{aligned}&\Lambda_7(x,y,t)\\&=\left\{\left(\begin{array}{c}\frac{\left(1-\frac{16\eta_1\eta_3-5\eta_2^2}{16\eta_1\eta_3-4\eta_2^2}\right)\sqrt{\eta_1\left(4\eta_1\eta_3-\eta_2^2\right)}(k_3t+k_1x+k_2y)}{2\eta_1}\\ -E\left(\mathrm{sn}\left(\frac{\sqrt{\eta_1\left(4\eta_1\eta_3-\eta_2^2\right)}(k_3t+k_1x+k_2y)}{2\eta_1},\frac{\sqrt{16\eta_1\eta_3-5\eta_2^2}}{2\sqrt{4\eta_1\eta_3-\eta_2^2}}\right),\frac{\sqrt{16\eta_1\eta_3-5\eta_2^2}}{2\sqrt{4\eta_1\eta_3-\eta_2^2}}\right)\\ +\frac{\mathrm{dc}\left(\frac{\sqrt{\eta_1\left(4\eta_1\eta_3-\eta_2^2\right)}(k_3t+k_1x+k_2y)}{2\eta_1},\frac{\sqrt{16\eta_1\eta_3-5\eta_2^2}}{2\sqrt{4\eta_1\eta_3-\eta_2^2}}\right)\mathrm{sc}\left(\frac{\sqrt{\eta_1\left(4\eta_1\eta_3-\eta_2^2\right)}(k_3t+k_1x+k_2y)}{2\eta_1},\frac{\sqrt{16\eta_1\eta_3-5\eta_2^2}}{2\sqrt{4\eta_1\eta_3-\eta_2^2}}\right)}{\mathrm{nc}\left(\frac{\sqrt{\eta_1\left(4\eta_1\eta_3-\eta_2^2\right)}(k_3t+k_1x+k_2y)}{2\eta_1},\frac{\sqrt{16\eta_1\eta_3-5\eta_2^2}}{2\sqrt{4\eta_1\eta_3-\eta_2^2}}\right)}\\ \times\frac{\rho_1(a\rho_2-\rho_1)(a\rho_2+\rho_1)a^2\eta_2^2}{4\left(-a^2\rho_2^2+\rho_1^2\right)\left(1-\frac{16\eta_1\eta_3-5\eta_2^2}{16\eta_1\eta_3-4\eta_2^2}\right)\sqrt{\eta_1\left(4\eta_1\eta_3-\eta_2^2\right)}}\\ \times\exp\left[-2vW(t)-2v^2t\right]\end{array}\right)\right\},\end{aligned}\tag{4.24}$$

$$\begin{aligned}&\Gamma_8(x,y,t)\\&=\left\{\begin{array}{c}\frac{a\kappa_2}{4}\sqrt{\frac{(a\rho_2-\rho_1)(a\rho_2+\rho_1)}{\zeta\kappa_1}}\\ \times nd\left(\frac{\sqrt{\left(16\kappa_1\kappa_3-5\kappa_2^2\right)\kappa_1}}{4\kappa_1}(\rho_1x+\rho_2y-\rho_3t),\frac{2\sqrt{\left(4\kappa_1\kappa_3-\kappa_2^2\right)\left(16\kappa_1\kappa_3-5\kappa_2^2\right)}}{\left(16\kappa_1\kappa_3-5\kappa_2^2\right)}\right)\end{array}\right\}\\&\times\exp\left[-vW(t)-v^2t+i(k_1x+k_2y+k_3t)\right].\end{aligned}\tag{4.25}$$

$$\begin{aligned}&\Lambda_8(x,y,t)\\&=\left\{\left(\begin{array}{c}E\left(\mathrm{sn}\left(\frac{\sqrt{\kappa_1\left(16\kappa_1\kappa_3-5\kappa_2^2\right)}(tk_3+xk_1+yk_2)}{4\kappa_1},\frac{2\sqrt{4\kappa_1\kappa_3-\kappa_2^2}}{\sqrt{16\kappa_1\kappa_3-5\kappa_2^2}}\right),\frac{2\sqrt{4\kappa_1\kappa_3-\kappa_2^2}}{\sqrt{16\kappa_1\kappa_3-5\kappa_2^2}}\right)\\ 4\left(4\kappa_1\kappa_3-\kappa_2^2\right)\mathrm{sd}\left(\frac{\sqrt{\kappa_1\left(16\kappa_1\kappa_3-5\kappa_2^2\right)}(tk_3+xk_1+yk_2)}{4\kappa_1},\frac{2\sqrt{4\kappa_1\kappa_3-\kappa_2^2}}{\sqrt{16\kappa_1\kappa_3-5\kappa_2^2}}\right)\\ \times\mathrm{cd}\left(\frac{\sqrt{\kappa_1\left(16\kappa_1\kappa_3-5\kappa_2^2\right)}(tk_3+xk_1+yk_2)}{4\kappa_1},\frac{2\sqrt{4\kappa_1\kappa_3-\kappa_2^2}}{\sqrt{16\kappa_1\kappa_3-5\kappa_2^2}}\right)\\ -\frac{}{\left(16\kappa_1\kappa_3-5\kappa_2^2\right)\mathrm{nd}\left(\frac{\sqrt{\kappa_1\left(16\kappa_1\kappa_3-5\kappa_2^2\right)}(tk_3+xk_1+yk_2)}{4\kappa_1},\frac{2\sqrt{4\kappa_1\kappa_3-\kappa_2^2}}{\sqrt{16\kappa_1\kappa_3-5\kappa_2^2}}\right)}\\ \times\frac{\kappa_2\rho_1(a\rho_2-\rho_1)(a\rho_2+\rho_1)a^2}{2\left(-a^2\rho_2^2+\rho_1^2\right)\left(1-\frac{4\left(4\kappa_1\kappa_3-\kappa_2^2\right)}{16\kappa_1\kappa_3-5\kappa_2^2}\right)\sqrt{\kappa_1\left(16\kappa_1\kappa_3-5\kappa_2^2\right)}}\\ \times\exp\left[-2vW(t)-2v^2t\right]\end{array}\right)^2\right\}.\end{aligned}\tag{4.26}$$

Sub-condition (1.5). For $\kappa_1 > 0$, and $(16\kappa_1\kappa_3 - 5\kappa_2^2) < 0$, then we obtain

$$\Gamma_9(x,y,t) = \left\{ \begin{array}{c} \frac{a\kappa_2}{4}\sqrt{\frac{(a\rho_2-\rho_1)(a\rho_2+\rho_1)}{\zeta\kappa_1}} \\ \times ns\left(\frac{\kappa_2}{4\sqrt{\kappa_1}}(\rho_1 x+\rho_2 y-\rho_3 t), \frac{\sqrt{-\left(16\kappa_1\kappa_3-5\kappa_2^2\right)}}{\kappa_2}\right) \end{array} \right\} \times \exp\left[-vW(t) - v^2 t + i(k_1 x + k_2 y + k_3 t)\right], \tag{4.27}$$

$$\Gamma_{11}(x,y,t) = \left\{ \begin{array}{c} \frac{a\sqrt{(-16\kappa_1\kappa_3+5\kappa_2^2)}}{4}\sqrt{\frac{(a\rho_2-\rho_1)(a\rho_2+\rho_1)}{\zeta\kappa_1}} \\ \times sn\left(\frac{\kappa_2}{4\sqrt{\kappa_1}}(\rho_1 x+\rho_2 y-\rho_3 t), \frac{\sqrt{-\left(16\kappa_1\kappa_3-5\kappa_2^2\right)}}{\kappa_2}\right) \end{array} \right\} \times \exp\left[-vW(t) - v^2 t + i(k_1 x + k_2 y + k_3 t)\right], \tag{4.31}$$

$$\Lambda_9(x,y,t) = \left\{ \left(\begin{array}{c} \frac{\kappa_2(tk_3+xk_1+yk_2)}{4\sqrt{\kappa_1}} - E\left(\mathrm{sn}\left(\frac{\kappa_2(tk_3+xk_1+yk_2)}{4\sqrt{\kappa_1}}, \frac{\sqrt{-16\kappa_1\kappa_3+5\kappa_2^2}}{\kappa_2}\right), \frac{\sqrt{-16\kappa_1\kappa_3+5\kappa_2^2}}{\kappa_2}\right) \\ -\frac{\mathrm{ds}\left(\frac{\kappa_2(tk_3+xk_1+yk_2)}{4\sqrt{\kappa_1}}, \frac{\sqrt{-16\kappa_1\kappa_3+5\kappa_2^2}}{\kappa_2}\right)\mathrm{cs}\left(\frac{\kappa_2(tk_3+xk_1+yk_2)}{4\sqrt{\kappa_1}}, \frac{\sqrt{-16\kappa_1\kappa_3+5\kappa_2^2}}{\kappa_2}\right)}{\mathrm{ns}\left(\frac{\kappa_2(tk_3+xk_1+yk_2)}{4\sqrt{\kappa_1}}, \frac{\sqrt{-16\kappa_1\kappa_3+5\kappa_2^2}}{\kappa_2}\right)} \\ \times\frac{\rho_1(a\rho_2-\rho_1)(a\rho_2+\rho_1)a^2\kappa_2}{2\left(-a^2\rho_2^2+\rho_1^2\right)\sqrt{\kappa_1}} \\ \times\exp\left[-2vW(t) - 2v^2 t\right] \end{array} \right) \right\}, \tag{4.28}$$

$$\Gamma_{10}(x,y,t) = \left\{ \begin{array}{c} \frac{a\sqrt{(-16\kappa_1\kappa_3+5\kappa_2^2)}}{4}\sqrt{\frac{(a\rho_2-\rho_1)(a\rho_2+\rho_1)}{\zeta\kappa_1}} \\ \times ns\left(\frac{\sqrt{-\kappa_1\left(16\kappa_1\kappa_3-5\kappa_2^2\right)}}{4\kappa_1}(\rho_1 x+\rho_2 y-\rho_3 t), \frac{\kappa_2}{\sqrt{-\left(16\kappa_1\kappa_3-5\kappa_2^2\right)}}\right) \end{array} \right\} \times \exp\left[-vW(t) - v^2 t + i(k_1 x + k_2 y + k_3 t)\right], \tag{4.29}$$

$$\Lambda_{10}(x,y,t) = \left\{ \left(\begin{array}{c} \frac{\sqrt{-\kappa_1\left(16\kappa_1\kappa_3-5\kappa_2^2\right)}(tk_3+xk_1+yk_2)}{4\kappa_1} \\ -E\left(\mathrm{sn}\left(\frac{\sqrt{-\kappa_1\left(16\kappa_1\kappa_3-5\kappa_2^2\right)}(tk_3+xk_1+yk_2)}{4\kappa_1}, \frac{\mathrm{I}\kappa_2}{\sqrt{16\kappa_1\kappa_3-5\kappa_2^2}}\right), \frac{\mathrm{I}\kappa_2}{\sqrt{16\kappa_1\kappa_3-5\kappa_2^2}}\right) \\ -\frac{\mathrm{ds}\left(\frac{\sqrt{-\kappa_1\left(16\kappa_1\kappa_3-5\kappa_2^2\right)}(tk_3+xk_1+yk_2)}{4\kappa_1}, \frac{\mathrm{I}\kappa_2}{\sqrt{16\kappa_1\kappa_3-5\kappa_2^2}}\right)\times\mathrm{cs}\left(\frac{\sqrt{-\kappa_1\left(16\kappa_1\kappa_3-5\kappa_2^2\right)}(tk_3+xk_1+yk_2)}{4\kappa_1}, \frac{\mathrm{I}\kappa_2}{\sqrt{16\kappa_1\kappa_3-5\kappa_2^2}}\right)}{\mathrm{ns}\left(\frac{\sqrt{-\kappa_1\left(16\kappa_1\kappa_3-5\kappa_2^2\right)}(tk_3+xk_1+yk_2)}{4\kappa_1}, \frac{\mathrm{I}\kappa_2}{\sqrt{16\kappa_1\kappa_3-5\kappa_2^2}}\right)} \\ \times\frac{\rho_1(a\rho_2-\rho_1)(a\rho_2+\rho_1)a^2\left(-16\kappa_1\kappa_3+5\kappa_2^2\right)}{2\left(-a^2\rho_2^2+\rho_1^2\right)\sqrt{-\kappa_1\left(16\kappa_1\kappa_3-5\kappa_2^2\right)}} \\ \times\exp\left[-2vW(t) - 2v^2 t\right] \end{array} \right) \right\}, \tag{4.30}$$

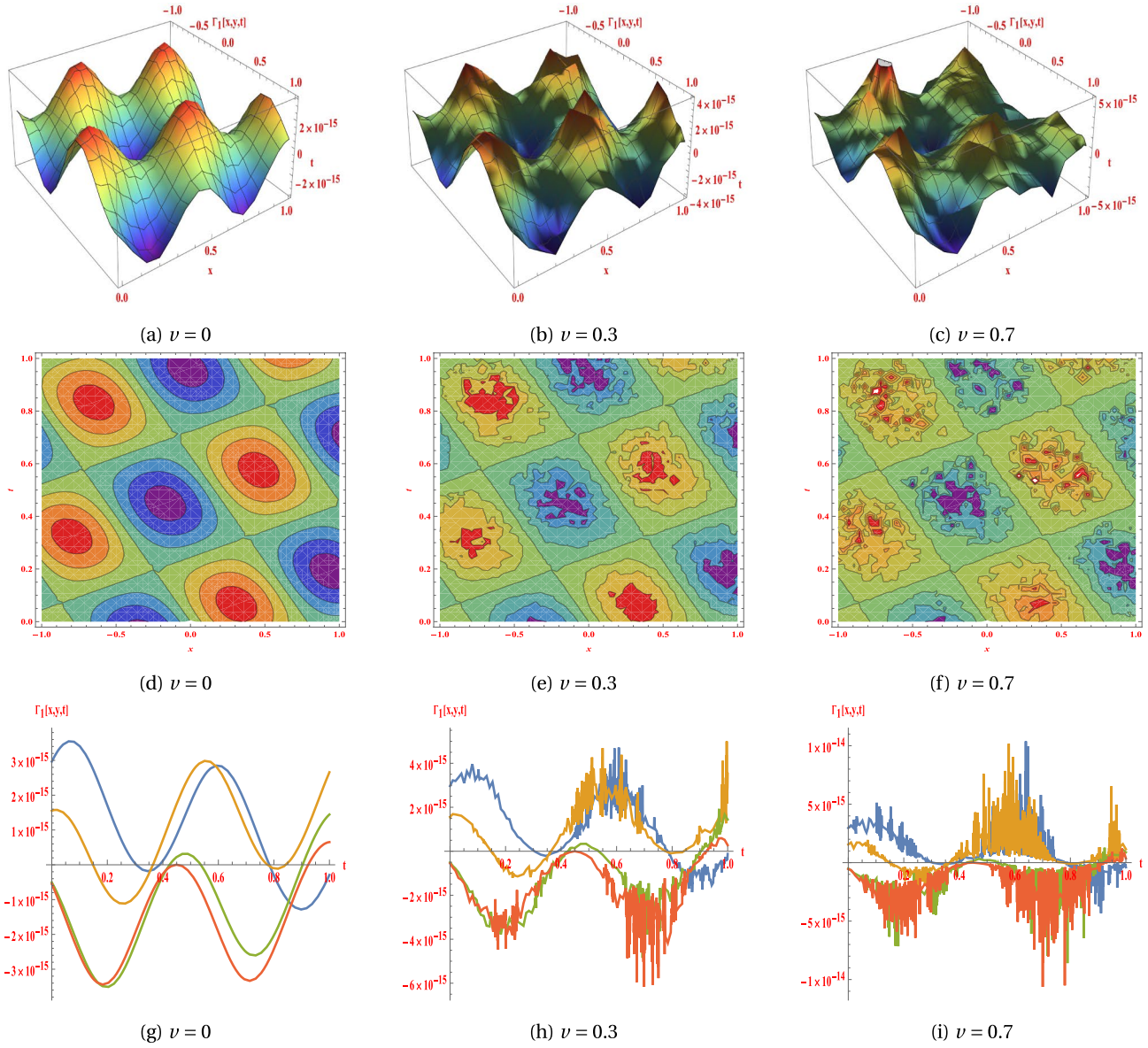

(a) $\upsilon = 0$ (b) $\upsilon = 0.3$ (c) $\upsilon = 0.7$

(d) $\upsilon = 0$ (e) $\upsilon = 0.3$ (f) $\upsilon = 0.7$

(g) $\upsilon = 0$ (h) $\upsilon = 0.3$ (i) $\upsilon = 0.7$

Fig. 1 The 3D, contour, and 2D plots for the real part of the periodic wave solution, $\Gamma_1(x, y, t)$ in Eq.(4.11) when $\kappa_1 = -1.1, \kappa_2 = 2, \kappa_3 = -3$, $k_1 = 4, k_3 = 5, \zeta = 0.1, y = 2, a = 0.5, \rho_1 = 1, \rho_2 = 6, \rho_3 = 5$

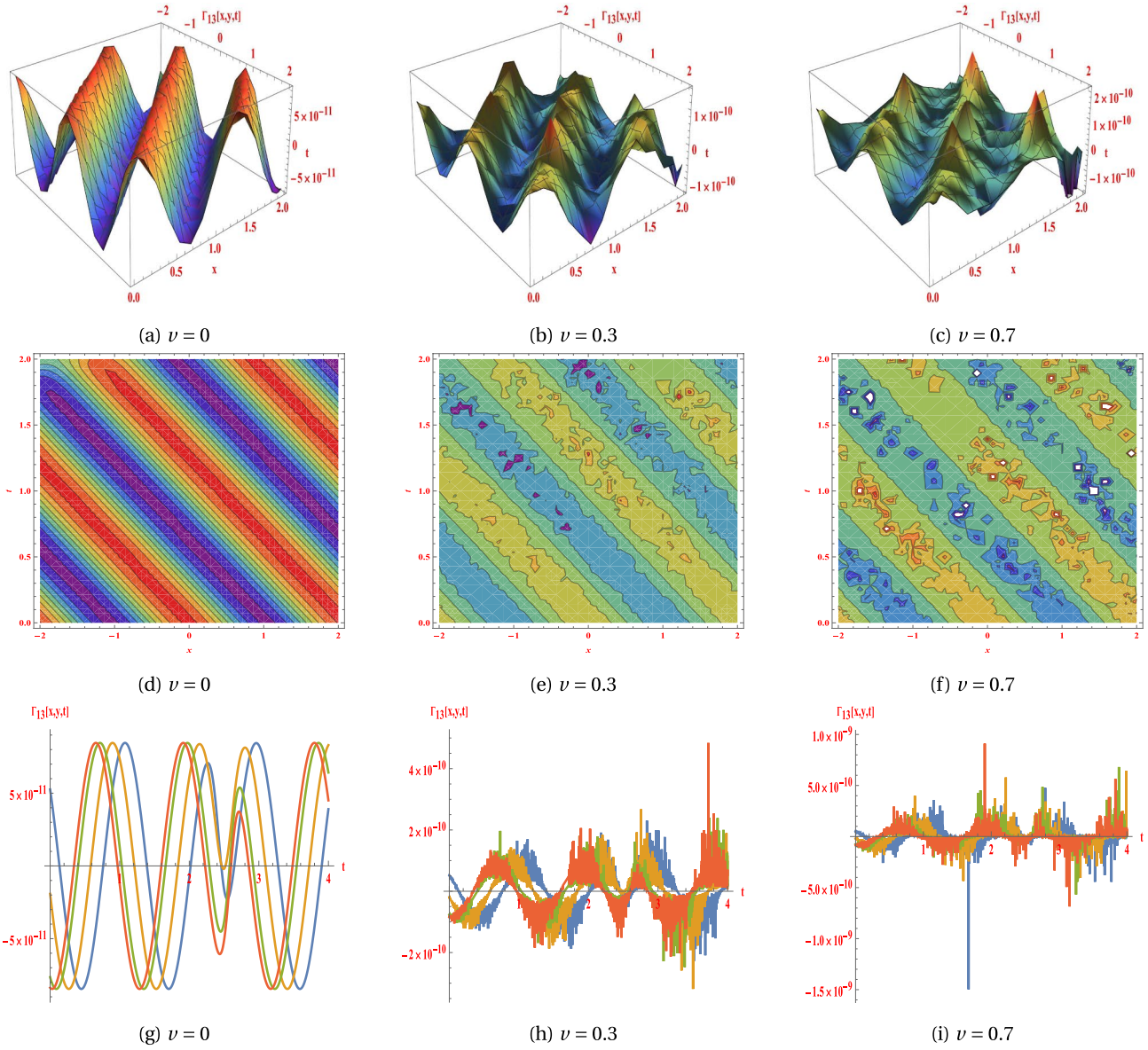

(a) $\upsilon = 0$ (b) $\upsilon = 0.3$ (c) $\upsilon = 0.7$

(d) $\upsilon = 0$ (e) $\upsilon = 0.3$ (f) $\upsilon = 0.7$

(g) $\upsilon = 0$ (h) $\upsilon = 0.3$ (i) $\upsilon = 0.7$

Fig. 2 The 3D, contour, and 2D plots for the real part of the dark soliton solution, $\Gamma_{13}(x, y, t)$ in Eq.(4.35) with $\kappa_1 = 2, \kappa_2 = 1, \kappa_3 = -4, k_1 = 3, k_3 = 5, \zeta = 7, y = 2, a = 1.5, \rho_1 = 1, \rho_2 = 6, \rho_3 = 5$

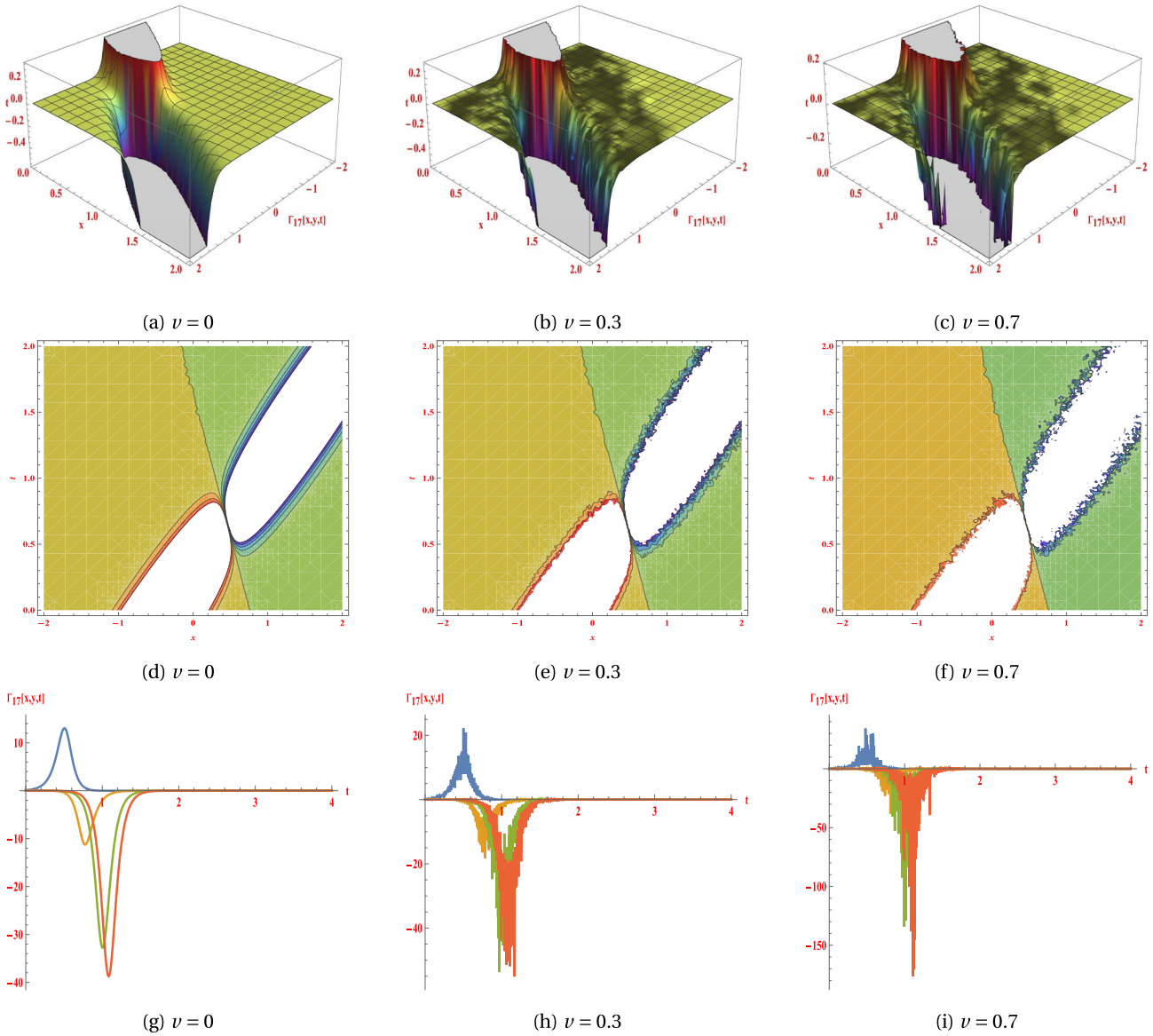

(a) $\upsilon = 0$ (b) $\upsilon = 0.3$ (c) $\upsilon = 0.7$

(d) $\upsilon = 0$ (e) $\upsilon = 0.3$ (f) $\upsilon = 0.7$

(g) $\upsilon = 0$ (h) $\upsilon = 0.3$ (i) $\upsilon = 0.7$

Fig. 3 The 3D, contour, and 2D plots for the real part of the bright soliton solution, $\Gamma_{17}(x, y, t)$ in Eq.(4.43) when $\kappa_1 = -3$,$\kappa_2 = 2$,$\kappa_3 = 5$, $k_1 = 1.1$,$k_3 = 0.5$,$\zeta = 0.2$,$y = 2$,$a = 3$,$\rho_1 = 4$,$\rho_2 = 0.7$,$\rho_3 = 5$

$$\Lambda_{11}(x,y,t) = \left\{ \begin{array}{c} \left(\frac{\kappa_2(k_3t+k_1x+k_2y)}{4\sqrt{\kappa_1}} - E\left(\mathrm{sn}\left(\frac{\kappa_2(k_3t+k_1x+k_2y)}{4\sqrt{\kappa_1}}, \frac{\sqrt{-16\kappa_1\kappa_3+5\kappa_2^2}}{\kappa_2} \right), \frac{\sqrt{-16\kappa_1\kappa_3+5\kappa_2^2}}{\kappa_2} \right) \right) \\ \times \frac{\rho_1(a\rho_2-\rho_1)(a\rho_2+\rho_1)a^2\kappa_2}{2\left(-\rho_2^2a^2+\rho_1^2\right)\sqrt{\kappa_1}} \\ \times \exp\left[-2vW(t)-2v^2t\right] \end{array} \right\}, \tag{4.32}$$

$$\Gamma_{12}(x,y,t) = \left\{ \begin{array}{c} \frac{a\kappa_2}{4}\sqrt{\frac{(a\rho_2-\rho_1)(a\rho_2+\rho_1)}{\zeta\kappa_1}} \\ \times sn\left(\frac{\sqrt{-\kappa_1\left(16\kappa_1\kappa_3-5\kappa_2^2\right)}}{4\kappa_1}(\rho_1x+\rho_2y-\rho_3t), \frac{\kappa_2}{\sqrt{-\left(16\kappa_1\kappa_3-5\kappa_2^2\right)}} \right) \end{array} \right\} \\ \times \exp\left[-vW(t)-v^2t+i(k_1x+k_2y+k_3t)\right], \tag{4.33}$$

$$\Lambda_{12}(x,y,t) = \left\{ \begin{array}{c} -\left(\begin{array}{c} \frac{\sqrt{-\kappa_1\left(16\kappa_1\kappa_3-5\kappa_2^2\right)}(tk_3+xk_1+yk_2)}{4\kappa_1} \\ -E\left(\mathrm{sn}\left(\frac{\sqrt{-\kappa_1\left(16\kappa_1\kappa_3-5\kappa_2^2\right)}(tk_3+xk_1+yk_2)}{4\kappa_1}, \frac{\mathrm{I}\kappa_2}{\sqrt{16\kappa_1\kappa_3-5\kappa_2^2}} \right), \frac{\mathrm{I}\kappa_2}{\sqrt{16\kappa_1\kappa_3-5\kappa_2^2}} \right) \end{array} \right) \\ \times \frac{\left(16\kappa_1\kappa_3-5\kappa_2^2\right)\rho_1(a\rho_2-\rho_1)(a\rho_2+\rho_1)a^2}{2\left(-a^2\rho_2^2+\rho_1^2\right)\sqrt{-\kappa_1\left(16\kappa_1\kappa_3-5\kappa_2^2\right)}} \\ \times \exp\left[-2vW(t)-2v^2t\right] \end{array} \right\}. \tag{4.34}$$

Condition (2). When $\kappa_4 = \frac{\kappa_2\left(4\kappa_1\kappa_3-\kappa_2^2\right)}{8\kappa_1^2}$, $\kappa_5 = \frac{\left(4\kappa_1\kappa_3-\kappa_2^2\right)^2}{64\kappa_1^3}$, then we acquire the next trigonometric and hyperbolic solutions:

Inserting Eq.(4.10) into Eq.(4.9) yields the desired solution to Eq.(1.1):

Sub-condition (2.1). For $\kappa_1 > 0$, and $(8\kappa_1\kappa_3 - 3\kappa_2^2) < 0$, then we discover

$$\Gamma_{13}(x,y,t) = \left\{ \begin{array}{c} \frac{a\sqrt{-8\kappa_1\kappa_3+3\kappa_2^2}}{4}\sqrt{\frac{(a\rho_2-\rho_1)(a\rho_2+\rho_1)}{\zeta\kappa_1}} \\ \times \tanh\left(\frac{\sqrt{-\kappa_1\left(8\kappa_1\kappa_3-3\kappa_2^2\right)}}{4\kappa_1}(\rho_1x+\rho_2y-\rho_3t) \right) \end{array} \right\} \\ \times \exp\left[-vW(t)-v^2t+i(k_1x+k_2y+k_3t)\right], \tag{4.35}$$

$$\Gamma_{14}(x,y,t) = \left\{ \begin{array}{c} \frac{a\sqrt{\left(-8\kappa_1\kappa_3+3\kappa_2^2\right)}}{4}\sqrt{\frac{(a\rho_2-\rho_1)(a\rho_2+\rho_1)}{\zeta\kappa_1}} \\ \times \coth\left(\frac{\sqrt{-\kappa_1\left(8\kappa_1\kappa_3-3\kappa_2^2\right)}}{4\kappa_1}(\rho_1x+\rho_2y-\rho_3t) \right) \end{array} \right\} \\ \times \exp\left[-vW(t)-v^2t+i(k_1x+k_2y+k_3t)\right], \tag{4.37}$$

$$\Lambda_{13}(x,y,t) = \left\{ \begin{array}{c} -\left(\begin{array}{c} \tanh\left(\frac{\sqrt{-\kappa_1\left(8\kappa_1\kappa_3-3\kappa_2^2\right)}(k_3t+k_1x+k_2y)}{4\kappa_1} \right) \\ +\frac{\ln\left(\tanh\left(\frac{\sqrt{-\kappa_1\left(8\kappa_1\kappa_3-3\kappa_2^2\right)}(k_3t+k_1x+k_2y)}{4\kappa_1} \right)-1 \right)}{2} - \frac{\ln\left(\tanh\left(\frac{\sqrt{-\kappa_1\left(8\kappa_1\kappa_3-3\kappa_2^2\right)}(k_3t+k_1x+k_2y)}{4\kappa_1} \right)+1 \right)}{2} \end{array} \right) \\ \times \frac{\rho_1(a\rho_2-\rho_1)(a\rho_2+\rho_1)a^2\left(-8\kappa_1\kappa_3+3\kappa_2^2\right)}{2\left(-a^2\rho_2^2+\rho_1^2\right)\sqrt{-\kappa_1\left(8\kappa_1\kappa_3-3\kappa_2^2\right)}} \\ \times \exp\left[-2vW(t)-2v^2t\right] \end{array} \right\}, \tag{4.36}$$

$$\Lambda_{14}(x,y,t) = \left\{ -\left(\begin{array}{c} \coth\left(\frac{\sqrt{-\kappa_1\left(8\kappa_1\kappa_3-3\kappa_2^2\right)}\,(k_3t+k_1x+k_2y)}{4\kappa_1}\right) \\ +\frac{\ln\left(\coth\left(\frac{\sqrt{-\kappa_1\left(8\kappa_1\kappa_3-3\kappa_2^2\right)}\,(k_3t+k_1x+k_2y)}{4\kappa_1}\right)-1\right)}{2} - \frac{\ln\left(\coth\left(\frac{\sqrt{-\kappa_1\left(8\kappa_1\kappa_3-3\kappa_2^2\right)}\,(k_3t+k_1x+k_2y)}{4\kappa_1}\right)+1\right)}{2} \end{array} \right) \right\}. \quad (4.38)$$

$$\times \frac{\rho_1(a\rho_2-\rho_1)(a\rho_2+\rho_1)a^2\left(-8\kappa_1\kappa_3+3\kappa_2^2\right)}{2\left(-a^2\rho_2^2+\rho_1^2\right)\sqrt{-\kappa_1\left(8\kappa_1\kappa_3-3\kappa_2^2\right)}} \times \exp\left[-2vW(t)-2v^2t\right]$$

Sub-condition (2.2). For $\kappa_1 > 0$, and $(8\kappa_1\kappa_3 - 3\kappa_2^2) > 0$, then we yield

$$\Gamma_{15}(x,y,t) = \left\{ \begin{array}{c} \frac{a\sqrt{\left(8\kappa_1\kappa_3-3\kappa_2^2\right)}}{4}\sqrt{\frac{(a\rho_2-\rho_1)(a\rho_2+\rho_1)}{\zeta\kappa_1}} \\ \times \tan\left(\frac{\sqrt{\kappa_1\left(8\kappa_1\kappa_3-3\kappa_2^2\right)}}{4\kappa_1}(\rho_1x+\rho_2y-\rho_3t)\right) \end{array} \right\} \quad (4.39)$$

$$\times \exp\left[-vW(t)-v^2t+i(k_1x+k_2y+k_3t)\right],$$

$$\Gamma_{17}(x,y,t) = \left\{ \begin{array}{c} \frac{a\sqrt{-2\left(8\kappa_1\kappa_3-3\kappa_2^2\right)}}{4}\sqrt{\frac{(a\rho_2-\rho_1)(a\rho_2+\rho_1)}{\zeta\kappa_1}} \\ \times \operatorname{sech}\left(\frac{\sqrt{2\kappa_1\left(8\kappa_1\kappa_3-3\kappa_2^2\right)}}{4\kappa_1}(\rho_1x+\rho_2y-\rho_3t)\right) \end{array} \right\} \quad (4.43)$$

$$\times \exp\left[-vW(t)-v^2t+i(k_1x+k_2y+k_3t)\right],$$

$$\Lambda_{15}(x,y,t) = \left\{ \begin{array}{c} \left(\tan\left(\frac{\sqrt{\kappa_1\left(8\kappa_1\kappa_3-3\kappa_2^2\right)}\,(tk_3+xk_1+yk_2)}{4\kappa_1}\right) - \arctan\left(\tan\left(\frac{\sqrt{\kappa_1\left(8\kappa_1\kappa_3-3\kappa_2^2\right)}\,(tk_3+xk_1+yk_2)}{4\kappa_1}\right)\right)\right) \\ \times \frac{\rho_1(a\rho_2-\rho_1)(a\rho_2+\rho_1)a^2\left(8\kappa_1\kappa_3-3\kappa_2^2\right)}{2\left(-a^2\rho_2^2+\rho_1^2\right)\sqrt{\kappa_1\left(8\kappa_1\kappa_3-3\kappa_2^2\right)}} \\ \times \exp\left[-2vW(t)-2v^2t\right] \end{array} \right\}, \quad (4.40)$$

$$\Gamma_{16}(x,y,t) = \left\{ \begin{array}{c} \frac{a\sqrt{\left(8\kappa_1\kappa_3-3\kappa_2^2\right)}}{4}\sqrt{\frac{(a\rho_2-\rho_1)(a\rho_2+\rho_1)}{\zeta\kappa_1}} \\ \times \cot\left(\frac{\sqrt{\kappa_1\left(8\kappa_1\kappa_3-3\kappa_2^2\right)}}{4\kappa_1}(\rho_1x+\rho_2y-\rho_3t)\right) \end{array} \right\} \quad (4.41)$$

$$\times \exp\left[-vW(t)-v^2t+i(k_1x+k_2y+k_3t)\right],$$

$$\Lambda_{16}(x,y,t) = \left\{ -\left(\begin{array}{c} \cot\left(\frac{\sqrt{\kappa_1\left(8\kappa_1\kappa_3-3\kappa_2^2\right)}\,(tk_3+xk_1+yk_2)}{4\kappa_1}\right) - \frac{\pi}{2} \\ +\operatorname{arccot}\left(\cot\left(\frac{\sqrt{\kappa_1\left(8\kappa_1\kappa_3-3\kappa_2^2\right)}\,(tk_3+xk_1+yk_2)}{4\kappa_1}\right)\right) \end{array} \right) \right\}. \quad (4.42)$$

$$\times \frac{\rho_1(a\rho_2-\rho_1)(a\rho_2+\rho_1)a^2\left(8\kappa_1\kappa_3-3\kappa_2^2\right)}{2\left(-a^2\rho_2^2+\rho_1^2\right)\sqrt{\kappa_1\left(8\kappa_1\kappa_3-3\kappa_2^2\right)}} \times \exp\left[-2vW(t)-2v^2t\right]$$

Condition (3). When $\kappa_4 = \frac{\kappa_2\left(4\kappa_1\kappa_3-\kappa_2^2\right)}{8\kappa_1^2}$, $\kappa_5 = \frac{\kappa_2^2\left(16\kappa_1\kappa_3-5\kappa_2^2\right)^2}{256\kappa_1^3}$, then the following are the trigonometric and hyperbolic solutions:

Substituting Eq.(4.10) into Eq.(4.9), the comprehensive solution to Eq.(1.1) is achieved:

Sub-condition (3.1). For $\kappa_1 < 0$, and $(8\kappa_1\kappa_3 - 3\kappa_2^2) < 0$, then we reach

$$\Lambda_{17}(x,y,t) = \left\{ \begin{array}{c} \tanh\left(\frac{\sqrt{2}\,\sqrt{\kappa_1\left(8\kappa_1\kappa_3-3\kappa_2^2\right)}\,(tk_3+xk_1+yk_2)}{4\kappa_1}\right) \\ \times \frac{\rho_1(a\rho_2-\rho_1)(a\rho_2+\rho_1)a^2\left(-8\kappa_1\kappa_3+3\kappa_2^2\right)\sqrt{2}}{2\left(-a^2\rho_2^2+\rho_1^2\right)\sqrt{\kappa_1\left(8\kappa_1\kappa_3-3\kappa_2^2\right)}} \\ \times \exp\left[-2vW(t)-2v^2t\right] \end{array} \right\}. \quad (4.44)$$

Sub-condition (3.2). For $\kappa_1 > 0$, and $(8\kappa_1\kappa_3 - 3\kappa_2^2) > 0$, then we attain

$$\Gamma_{18}(x,y,t) = \left\{ \begin{array}{c} \frac{a\sqrt{2\left(8\kappa_1\kappa_3-3\kappa_2^2\right)}}{4}\sqrt{\frac{(a\rho_2-\rho_1)(a\rho_2+\rho_1)}{\zeta\kappa_1}} \\ \times \operatorname{csch}\left(\frac{\sqrt{2\kappa_1\left(8\kappa_1\kappa_3-3\kappa_2^2\right)}}{4\kappa_1}(\rho_1x+\rho_2y-\rho_3t)\right) \end{array} \right\} \quad (4.45)$$

$$\times \exp\left[-vW(t)-v^2t+i(k_1x+k_2y+k_3t)\right].$$

$$\Lambda_{18}(x,y,t) = \left\{ \begin{array}{c} -\coth\left(\frac{\sqrt{2}\,\sqrt{\kappa_1\left(8\kappa_1\kappa_3-3\kappa_2^2\right)}\,(k_3t+k_1x+k_2y)}{4\kappa_1}\right) \\ \times \frac{\rho_1(a\rho_2-\rho_1)(a\rho_2+\rho_1)a^2\left(8\kappa_1\kappa_3-3\kappa_2^2\right)\sqrt{2}}{2\left(-a^2\rho_2^2+\rho_1^2\right)\sqrt{\kappa_1\left(8\kappa_1\kappa_3-3\kappa_2^2\right)}} \\ \times \exp\left[-2vW(t)-2v^2t\right] \end{array} \right\}. \quad (4.46)$$

Sub-condition (3.3). For $\kappa_1 > 0$, and $(8\kappa_1\kappa_3 - 3\kappa_2^2) < 0$, then we reach

$$\Gamma_{19}(x,y,t) = \left\{ \begin{array}{c} \frac{a\sqrt{-2\left(8\kappa_1\kappa_3-3\kappa_2^2\right)}}{4}\sqrt{\frac{(a\rho_2-\rho_1)(a\rho_2+\rho_1)}{\zeta\kappa_1}} \\ \times \sec\left(\frac{\sqrt{-2\kappa_1\left(8\kappa_1\kappa_3-3\kappa_2^2\right)}}{4\kappa_1}(\rho_1 x+\rho_2 y-\rho_3 t)\right) \end{array} \right\} \times \exp\left[-vW(t)-v^2t+i(k_1x+k_2y+k_3t)\right], \tag{4.47}$$

$$\Lambda_{19}(x,y,t) = \left\{ \begin{array}{c} \tan\left(\frac{\sqrt{-2\kappa_1\left(8\kappa_1\kappa_3-3\kappa_2^2\right)}}{4\kappa_1}(tk_3+xk_1+yk_2)\right) \\ \times \frac{\rho_1(a\rho_2-\rho_1)(a\rho_2+\rho_1)a^2\left(-8\kappa_1\kappa_3+3\kappa_2^2\right)}{\left(-a^2\rho_2^2+\rho_1^2\right)\sqrt{-2\kappa_1\left(8\kappa_1\kappa_3-3\kappa_2^2\right)}} \\ \times \exp\left[-2vW(t)-2v^2t\right] \end{array} \right\}, \tag{4.48}$$

$$\Gamma_{20}(x,y,t) = \left\{ \begin{array}{c} \frac{a\sqrt{-2\left(8\kappa_1\kappa_3-3\kappa_2^2\right)}}{4}\sqrt{\frac{(a\rho_2-\rho_1)(a\rho_2+\rho_1)}{\zeta\kappa_1}} \\ \times \csc\left(\frac{\sqrt{-2\kappa_1\left(8\kappa_1\kappa_3-3\kappa_2^2\right)}}{4\kappa_1}(\rho_1 x+\rho_2 y-\rho_3 t)\right) \end{array} \right\} \times \exp\left[-vW(t)-v^2t+i(k_1x+k_2y+k_3t)\right], \tag{4.49}$$

$$\Lambda_{20}(x,y,t) = \left\{ \begin{array}{c} -\cot\left(\frac{\sqrt{-2\kappa_1\left(8\kappa_1\kappa_3-3\kappa_2^2\right)}(k_3t+k_1x+k_2y)}{4\kappa_1}\right) \\ \times \frac{\rho_1(a\rho_2-\rho_1)(a\rho_2+\rho_1)a^2\left(-8\kappa_1\kappa_3+3\kappa_2^2\right)}{\left(-a^2\rho_2^2+\rho_1^2\right)\sqrt{-2\kappa_1\left(8\kappa_1\kappa_3-3\kappa_2^2\right)}} \\ \times \exp\left[-2vW(t)-2v^2t\right] \end{array} \right\}. \tag{4.50}$$

By applying the phases of the method, we get the following Cluster for **Condition (4)**.

Cluster:

$$k_2 = \frac{\sqrt{\left(\kappa_3\rho_2^2a^4+\left(\kappa_3\rho_1^2-k_1^2\right)a^2-2k_3\right)}}{a^2},$$

$$\Upsilon_0 = 0, \quad \Upsilon_1 = a\sqrt{-\frac{-a^2\kappa_1\rho_2^2+\kappa_1\rho_1^2}{\zeta}}. \tag{4.51}$$

Condition (4). When $\kappa_2 = 0$, $\kappa_4 = 0$, $\kappa_5 = 0$, then we obtain exponential solutions as follows:

Inserting Eq.(4.51) into Eq.(4.9), the desired solution to Eq.(1.1) is attained:

$$\Gamma_{21}(x,y,t) = \left\{ \frac{4a\varrho\kappa_3\sqrt{\frac{\kappa_1(a\rho_2-\rho_1)(a\rho_2+\rho_1)}{\zeta}}}{\left(4\varrho^2\exp\left[\sqrt{\kappa_3}(\rho_1x+\rho_2y-\rho_3t)\right]-\kappa_1\kappa_3\exp\left[-\sqrt{\kappa_3}(\rho_1x+\rho_2y-\rho_3t)\right]\right)} \right\} \times \exp\left[-vW(t)-v^2t+i(k_1x+k_2y+k_3t)\right], \tag{4.52}$$

$$\Lambda_{21}(x,y,t) = \left\{ \begin{array}{c} -\frac{4\rho_1(a\rho_2-\rho_1)^2\kappa_1a^2\kappa_3^3}{\left(-a^2\rho_2^2+\rho_1^2\right)\left(4\varrho^2\left(e^{\sqrt{\kappa_3}(k_3t+k_1x+k_2y)}\right)^2-\kappa_1\kappa_3\right)} \\ \times \exp\left[-2vW(t)-2v^2t\right] \end{array} \right\}. \tag{4.53}$$

Sub-condition (4.1). For $\kappa_1 = -\frac{4\varrho^2}{\kappa_3}$, then we discover

$$\Gamma_{22}(x,y,t) = \left\{ \frac{\sqrt{-\frac{\varrho^2(a\rho_2-\rho_1)(a\rho_2+\rho_1)}{\zeta\kappa_3}}a\kappa_3}{\varrho}\operatorname{sech}\left(\sqrt{\kappa_3}(\rho_1x+\rho_2y-\rho_3t)\right) \right\} \times \exp\left[-vW(t)-v^2t+i(k_1x+k_2y+k_3t)\right], \tag{4.54}$$

$$\Lambda_{22}(x,y,t) = \left\{ \begin{array}{c} -\frac{\tanh\left(\sqrt{\kappa_3}(k_3t+k_1x+k_2y)\right)2\rho_1(a\rho_2-\rho_1)^2\sqrt{\kappa_3}a^2}{-a^2\rho_2^2+\rho_1^2} \\ \times \exp\left[-2vW(t)-2v^2t\right] \end{array} \right\}. \tag{4.55}$$

Sub-condition (4.2). For $\kappa_1 = \frac{4\varrho^2}{\kappa_3}$, then we obtain

$$\Gamma_{23}(x,y,t) = \left\{ -\frac{\sqrt{\frac{\varrho^2(a\rho_2-\rho_1)(a\rho_2+\rho_1)}{\zeta\kappa_3}}a\kappa_3}{\varrho}\operatorname{csch}\left(\sqrt{\kappa_3}(\rho_1x+\rho_2y-\rho_3t)\right) \right\} \times \exp\left[-vW(t)-v^2t+i(k_1x+k_2y+k_3t)\right], \tag{4.56}$$

$$\Lambda_{23}(x,y,t) = \left\{ \begin{array}{c} -\frac{\coth\left(\sqrt{\kappa_3}(k_3t+xk_1+yk_2)\right)2\rho_1(a\rho_2-\rho_1)^2\sqrt{\kappa_3}a^2}{-a^2\rho_2^2+\rho_1^2} \\ \times \exp\left[-2vW(t)-2v^2t\right] \end{array} \right\}. \tag{4.57}$$

5 Graphical Discussion

In this part, the noise effects in the stochastic soliton solutions derived from the SDSM model using the Kumar-Malik approach are physically described. This method gives us exact solitary wave and soliton solutions and is a mathematical derivation that is efficient and simple to compute. Various kinds of solitons with dark, bright, linked, and periodic waves have been effectively produced. Using various parameter values, several solutions are displayed in 3D, contour, and 2D plots. The plots were generated using Mathematica software, by considering either the real part of the solutions. Figure 1 shows a periodic wave solution. A dark soliton solution is obtained in Fig. 2. A bright soliton solution is depicted in Fig. 3. To show the noise effect, different noise strengths were used. Also, the sub-figure plotted

for $v = 0$ on the left, the sub-figure plotted for $v = 0.3$ in the middle, and the sub-figure plotted for $v = 0.7$ on the right show different behaviour for different values of noise strength. Fig. 1 illustrates the influence of the stochastic parameter v on the real part of the solution $\Gamma_1(x, y, t)$ in Eq. (4.11), merging 3D, contour, and 2D cross-section plots. Subfigures (a)-(c) illustrate the evolution of the wave surface in 3D as v increases from 0 to 0.7, showing a clear transition from smooth, periodic (when $v = 0$) to increasingly disordered and less regular structures typical of stochastic disturbance. The corresponding contour plots (d)-(f) confirm this explanation, where contour lines become progressively fragmented and complex with growing v, indicating the sensitivity of the model to noise. Subplots (g)-(i) show 2D slices of the solution in specific directions, showing wave profile warping under noise and capturing the onset of instability. These plots together provide crucial information on how stochastic fluctuations can ruin coherent wave structures and are a useful tool for exploring real systems where environmental randomness affects wave propagation, like at fluid boundaries, in optical waves, or in plasma physics. Figure 2 illustrates the impact of varying stochastic intensity v on the structure of the real part of $\Gamma_{13}(x, y, t)$, derived from Eq. (4.35), for fixed values of the parameters. The 3D surfaces in subfigures (a)–(c) illustrate a deformation from a very ordered oscillatory state at $v = 0$ to a more deformed and irregular wave structure at $v = 0.3$ and $v = 0.7$. This illustrates the destruction of spatial coherence by noise and the amplification of localized instabilities. This tendency is confirmed by the contour plots in (d)–(f), where nicely ordered wavefronts become increasingly disordered and lose symmetry when noise is added, reflecting the loss of regularity. The 2D projections in (g)–(i) highlight steep gradients and phase discontinuities created by randomness, reflecting noise-induced modulation effects. These behaviors signify that the system is extremely sensitive to stochastic perturbations; thus, the model is suitable for investigating wave evolution under noisy environments such as electromagnetic wave propagation in disordered media or perturbations in shallow water waves under environmental influences. The last Fig. (3) illustrates the real part of a principal function or system response versus the parameter v, which indicates major physical or mathematical characteristics such as stability transitions, bifurcations, or phase transitions. The top row's 3D plots reveal global geometry and feature changes in the landscape of the function as v is increased, while the middle contour plots depict level set change, indicating feature creation or elimination, like peaks or singularities. The bottom row's cross-sectional views further reveal localized changes, giving insight into how specific features emerge or perish with v. Cumulatively, these images are valuable to understanding the system's behavior in different regimes, providing both qualitative and quantitative data on the underlying dynamics or mathematical features as the parameter varies. The visualization of the solutions obtained from the SDSM model allows us to understand how stochastic effects preserve the shape and speed of solitons in optical systems, while also illustrating how random effects influence the chaos in wave propagation.

6 Comparison with Previous Literature

In order to put the novelty and range of the equations considered in the present study into perspective, we situate our stochastic variant of the Davey–Stewartson (DS) model within the context of nearby recent developments in the literature.

In Madani et al. [50], the authors have considered stochastic extensions of the DS system by adding white noise terms to the evolution equations and analyzing their effect on the usual bright and dark soliton solutions. This was accomplished by. While their treatment effectively maintained the classical form of the DS equations with small noisy terms, our model includes noise in a more generalized form, affecting dispersive and nonlinear terms simultaneously, leading to more dynamically rich and unstable solution behavior.

Tariq et al. [43] focused on the sensitivity and chaotic dynamics of a DS system under random excitation. Their Lyapunov-based methodology gave precedence to the stability features and bifurcation points of formed waveforms. By comparison, our formulation offers a broader set of exact analytical solutions–including singular periodic waves and bifurcated structures–yielding explicit closed-form expressions in random environments, which were not presented in their sensitivity-based framework.

In another direction, Mohammed et al. [52] examined the influence of fractional derivatives and Brownian motion on the DS system, namely through a stochastic fractional framework. Their use of Caputo-type derivatives revealed long-memory effects in wave profiles. Our study differs by remaining in the conformable stochastic domain but deriving new classes of exact solutions without resorting to fractional-order operators, thereby minimizing the mathematical handling while preserving complexity in solution form.

Al-Askar et al. [42] showed that multiplicative Brownian motion has the effect of stabilizing certain stochastic DS solutions. While their study emphasized the role of stochasticity as a control strategy, our model shows the opposite side–showing how stochastic effects can enhance solution irregularity, instability, and bifurcation, especially in complex wave fields, and thus reflect chaotic evolution and dispersion under noise more evidently.

Briefly, the stochastic DS model explored in this study introduces a structurally distinct set of governing equations where randomness is not limited to perturbative control but is mainly accountable for structuring the dynamics. The resulting analytical solutions are more diverse and physically rich than those reported in the earlier literature, which underscores the originality of our contribution.

7 Conclusion

In this paper, we analyzed the SDSM model in a random environment. It is a two-dimensional integrable model, which is a higher-dimensional generalization of the nonlinear Schrödinger equation. Numerous applications of this equation can be found in nonlinear optics, hydrodynamics, plasma theory, and other fields. In this study, we use the Kumar-Malik approach for the first time to obtain innovative stochastic soliton solutions for the SDSM model. The real and imaginary parts of the complex function of the profile pulse are represented by the two integral equations we obtained for the model under consideration using the Kumar-Malik approach. Four various scenarios of solutions to the SDSM model using the Kumar-Malik approach, which uses 23 soliton solutions, have been discussed. This novel approach produced a variety of stochastic soliton solutions, and they demonstrated robustness across a range of parameter values, including periodic, bright, singular, and dark solitons. We also aimed to demonstrate the potential applications of these methods in real-world applications by deriving further solutions expressed in terms of Jacobi elliptic, trigonometric, hyperbolic, and exponential functions. Using 3D, contour, and 2D plots for varying noise strength values, we demonstrated the dynamic behaviors of the solutions in order to clarify the impact of Brownian motion on the numerous generated solutions. These illustrations give a physical explanation of the behavior of solitons and aid in our understanding of their dynamics. The results show that the above-described approach is both trustworthy and effective. Additionally, Maple software is used to confirm that all results are accurate. As far as we are aware, the discussion and conclusions presented in this work are new, important, and creative in a number of scientific domains where the SDSM model is used to depict physical phenomena. In the future, we will study stochastic-type equations to investigate new nonlinear models in a range of applied scientific fields.

Author Contributions F.N.K.S.: Formal analysis, Software, Methodology; B.K.: Validation, Methodology; K.K.A.: Methodology, Resources, Writing-review & editing.

Funding Not applicable.

Data Availability The datasets used and/or analysed during the current study are available from the corresponding author on reasonable request.

Declarations

Conflict of interest The authors declare that there is no Conflict of interest.

Ethical Approval Not applicable.

Consent to Participate Not applicable.

Consent for Publication Not applicable.

References

1. Kumar S, Niwas M (2021) Exact closed-form solutions and dynamics of solitons for a (2+1)-dimensional universal hierarchy equation via Lie approach. Pramana 95(4):195
2. Khalifa A, Ahmed H, Ahmed KK (2024) Construction of exact solutions for a higher-order stochastic modified Gerdjikov–Ivanov model using the IMETF method. Physica Scripta
3. Shakir AP, Sulaiman TA, Ismael HF, Shah NA, Eldin SM (2023) Multiple fusion solutions and other waves behavior to the Broer–Kaup–Kupershmidt system. Alex Eng J 74:559–567
4. Yasin MW, Ahmed N, Iqbal MS, Raza A, Rafiq M, Eldin EMT, Khan I (2023) Spatio-temporal numerical modeling of stochastic predator-prey model. Sci Rep 13(1):1990
5. Murad MAS, Mustafa MA, Younas U, Emadifar H, Khalifa AS, Mohammed WW, Ahmed KK (2025) Soliton solutions to the generalized derivative nonlinear Schrödinger equation under the effect of multiplicative white noise and conformable derivative. Sci Rep 15(1):1–15
6. Ahmed KK, Ahmed HM, Shehab MF, Khalil TA, Emadifar H, Rabie WB (2024) Characterizing stochastic solitons behavior in (3+ 1)-dimensional Schrödinger equation with Cubic-Quintic nonlinearity using improved modified extended tanh-function scheme. Phys Open 21:100233
7. Kumar S, Rani S (2021) Invariance analysis, optimal system, closed-form solutions and dynamical wave structures of a (2+ 1)-dimensional dissipative long wave system. Phys Scr 96(12):125202
8. Kumar S, Rani S (2022) Symmetries of optimal system, various closed-form solutions, and propagation of different wave profiles for the Boussinesq–Burgers system in ocean waves. Phys Fluids, 34(3)
9. Rani S, Kumar S (2025) Dynamics of soliton solutions and various evolving formations of the Jaulent–Miodek and Zakharov–Kuzetsov equations utilizing the newly proposed extended generalized approach. Qual Theory Dyn Syst 24(2):101
10. Li Z, Liu C (2024) Chaotic pattern and traveling wave solution of the perturbed stochastic nonlinear Schrödinger equation with generalized anti-cubic law nonlinearity and spatio-temporal dispersion. Results Phys 56:107305
11. Mohammed WW, Al-Askar FM (2024) New stochastic solitary solutions for the modified Korteweg-de Vries equation with stochastic term/random variable coefficients. AIMS Math 9(8):20467–20481

12. Luo J (2024) Traveling wave solution and qualitative behavior of fractional stochastic Kraenkel–Manna–Merle equation in ferromagnetic materials. Sci Rep 14(1):12990
13. Arshad M, Aldosary SF, Batool S, Hussain I, Hussain N (2024) Exploring fractional-order new coupled Korteweg-de Vries system via improved Adomian decomposition method. PLoS ONE 19(5):e0303426
14. Noor S, Alshehry AS, Shafee A, Shah R (2024) Families of propagating soliton solutions for (3+ 1)-fractional Wazwaz–Benjamin-Bona–Mahony equation through a novel modification of modified extended direct algebraic method. Phys Scr 99(4):045230
15. Zayed EM, Alurrfi KA (2017) Solitons and other solutions for two nonlinear Schrödinger equations using the new mapping method. Optik 144:132–148
16. Abdou MA (2007) The extended F-expansion method and its application for a class of nonlinear evolution equations. Chaos, Solitons Fractals 31(1):95–104
17. Wang M, Li X (2005) Extended F-expansion method and periodic wave solutions for the generalized Zakharov equations. Phys Lett A 343(1–3):48–54
18. Sahoo M, Chakraverty S (2024) Riccati–Bernoulli sub-ode method-based exact solution of new coupled Konno–Oono equation. Int J Modern Phys B, 2440028
19. Shehata MS (2016) A new solitary wave solution of the perturbed nonlinear Schrodinger equation using a Riccati–Bernoulli Sub-ODE method. Int J Phys Sci 11(6):80–84
20. Foroutan M, Manafian J, Zamanpour I (2018) Soliton wave solutions in optical metamaterials with anti-cubic law of nonlinearity by ITEM. Optik 164:371–379
21. Alam MN (2023) An analytical method for finding exact solutions of a nonlinear partial differential equation arising in electrical engineering. Open J Mathe Sci 7(1):10–18
22. Zhang S, Tong JL, Wang W (2008) A generalized (G' G)-expansion method for the mKdV equation with variable coefficients. Phys Lett A 372(13):2254–2257
23. Naher H (2015) New approach of (G'/G)-expansion method and new approach of generalized (G'/G)-expansion method for ZKBBM equation. J Egyptian Math Soc 23(1):42–48
24. Rahman MM, Islam SM, Hoque A (2025) Investigations of soliton structures and dynamical behaviors of the Westervelt equation with two analytical techniques, AIP Adv, 15(5)
25. Arafat SY, Rahman MM, Karim MF, Amin MR (2023) Wave profile analysis of the (2+ 1)-dimensional Konopelchenko–Dubrovsky model in mathematical physics. Partial Differ Equ Appl Math 8:100573
26. Dey P, Sadek LH, Tharwat MM, Sarker S, Karim R, Akbar MA, Elazab NS, Osman MS (2024) Soliton solutions to generalized (3+ 1)-dimensional shallow water-like equation using the expansion method. Arab J Basic Appl Sci 31(1):121–131
27. Islam SR, Islam ME, Akbar MA, Kumar D (2025) The stretch coordinate effect, bifurcation, and stability analysis of the nonlinear Hamiltonian amplitude equation, Partial Differ Equ Appl Math, 101126
28. Arafat SM, Saklayen MA, Islam SM (2025) Analyzing diverse soliton wave profiles and bifurcation analysis of the (3+ 1)-dimensional mKdV–ZK model via two analytical schemes, AIP Adv, 15(1)
29. Yiasir AS, Asif M, Rayhanul IS, Saklayen MA, Rahman MM (2024) Investigating travelling wave solutions of the (2+ 1)-dimensional Boiti–Leon–Manna–Pempinelli equation through the two analytical techniques. Phys Scr 100(1):015285
30. Arafat SY, Islam SR (2024) Bifurcation analysis and soliton structures of the truncated M-fractional Kuralay-II equation with two analytical techniques. Alex Eng J 105:70–87
31. Islam SR (2024) Bifurcation analysis and soliton solutions to the doubly dispersive equation in elastic inhomogeneous Murnaghan's rod. Sci Rep 14(1):11428
32. Islam SR (2024) On the soliton structures of the (2+ 1)-dimensional long wave-short wave resonance interaction equation with two analytical techniques and its bifurcation analysis, GANIT J Bangladesh Math Soc, 44(1), 59-76
33. Rayhanul Islam SM, Yiasir Arafat SM, Inc M (2025) Exploring novel optical soliton solutions for the stochastic chiral nonlinear Schrödinger equation: Stability analysis and impact of parameters, J Nonlinear Opt Phys Mater, 34(05), 2450009
34. Islam SR (2024) Bifurcation analysis and exact wave solutions of the nano-ionic currents equation: Via two analytical techniques. Results Phys 58:107536
35. Islam SR, Arafat SY, Alotaibi H, Inc M (2024) Some optical soliton solutions with bifurcation analysis of the paraxial nonlinear Schrödinger equation. Opt Quant Electron 56(3):379
36. Khan MI, Faridi WA, Murad MAS, Iqbal M, Myrzakulov R, Umurzakhova Z (2025) The formation and propagation of soliton wave profiles for the Shynaray-IIa equation, Acta Mechanica et automatica, 19(1)
37. Alhefthi RK, Khan MI, Sabi'u J (2024) Solitary wave type solutions of nonlinear improved mKdV equation by modified techniques, Revista Mexicana de Física, 70(5 Sep-Oct), 051301-1
38. Khan MI, Khan A, Farooq A (2024) Analyzing the Kuralay-II equation: bifurcation, chaos, and sensitivity insights through conformable derivative and Jacobi elliptic function expansion. Phys Scr 99(9):095210
39. Farooq A, Ma WX, Khan MI (2024) Exploring exact solitary wave solutions of Kuralay-II equation based on the truncated M-fractional derivative using the Jacobi Elliptic function expansion method. Opt Quant Electron 56(7):1105
40. Ahmed KK, Ahmed HM, Badra NM, Mirzazadeh M, Rabie WB, Eslami M (2024) Diverse exact solutions to Davey–Stewartson model using modified extended mapping method. Nonlinear Analysis: Modelling and Control 29(5):983
41. Iqbal MS, Inc M (2024) Optical Soliton solutions for stochastic Davey–Stewartson equation under the effect of noise. Opt Quant Electron 56(7):1148
42. Al-Askar FM, Cesarano C, Mohammed WW (2022) Multiplicative Brownian motion stabilizes the exact stochastic solutions of the Davey–Stewartson equations. Symmetry 14(10): 2176
43. Tariq MM, Riaz MB, Kozubek T, Aziz-ur-Rehman M (2025) Exploring chaos and stability: dynamic insights into the stochastic Davey–Stewartson system through advanced sensitivity analysis. Model Earth Syst Environ 11(2):83
44. Qi J, Cui Q, Bai L, Sun Y (2024) Investigating exact solutions, sensitivity, and chaotic behavior of multi-fractional order stochastic Davey–Sewartson equations for hydrodynamics research applications. Chaos, Solitons Fractals 180:114491
45. Cheemaa N, Siddiqui HMA, Nazir B, Bekir A, Almehizia AA, Hussein HH (2025) Stability, sensitivity, chaotic behavior, and phase trajectories evaluation of the Davey–Stewartson stochastic equation. Nonlinear Dyn, 1-17
46. Sağlam FNK, Kopçasız B, Şenol M (2025) Abundant new soliton solutions to the Arshed-Biswas equation via two novel integrating schemes. Modern Phys Lett A, 40(19n20), 2550054
47. Kuldeep, Kaur L (2025) Hirota bilinear approach for exploring diverse variety of solutions to (2+ 1)-dimensional bidirectional Sawada–Kotera equation. Rom Rep Phys, 77(1)
48. Elbrolosy M, Elmandouh A (2025) Painlevé analysis, Lie symmetry and bifurcation for the dynamical model of radial dislocations in microtubules. Nonlinear Dyn, 1-16

49. Wang J, Wang L, Yangjie J (2025) Darboux transformations of nonlinear coupled equations and their solutions. J Nonlinear Math Phys 32(1):1–18
50. Madani YA, Hussain S, Almalahi MA, Muflh B, Aldwoah KA, Abdalla MY (2025) Comprehensive study of stochastic soliton solutions in nonlinear models with application to the Davey–Stewartson equations. Sci Rep 15(1):1–19
52. Mohammed WW, Al-Askar FM, El-Morshedy M (2023) Impacts of Brownian motion and fractional derivative on the solutions of the stochastic fractional Davey–Stewartson equations. Demonstratio Math 56(1):20220233